European Polymer Journal 108 (2018) 150–170

Contents lists available at ScienceDirect

European Polymer Journal

journal homepage: www.elsevier.com/locate/europolj

Biocompatible and electroconductive polyaniline-based biomaterials for electrical stimulation

Yaser Arteshi[a,b], Ayuob Aghanejad[a], Soodabeh Davaran[a,b], Yadollah Omidi[a,c,*]

[a] Research Center for Pharmaceutical Nanotechnology, Biomedicine Institute, Tabriz University of Medical Sciences, Tabriz, Iran
[b] Department of Medicinal Chemistry, Faculty of Pharmacy, Tabriz University of Medical Sciences, Tabriz, Iran
[c] Department of Pharmaceutics, Faculty of Pharmacy, Tabriz University of Medical Sciences, Tabriz, Iran

ARTICLE INFO

Keywords:
Polyaniline
Biomaterials
Electrical conductivity
Biocompatibility
Electrical stimulation

ABSTRACT

Polyaniline (PANI) involved materials have extended approved applications in different fields, including bio/chemical-sensors, electrical and electrochemical devices, electrochemically active membranes and stimuli-responsive systems. These materials have attracted most of the interest in the field of development of biomaterials for tissue engineering and drug delivery systems. PANI offers remarkable features such as the ease of synthesis, considerable electrical conductivity especially in the doped condition, simplicity in the modification to improve water processability and enhanced biocompatibility. An engineered PANI-based biomaterial can be applied in the process named the electrical stimulation (ES), in which cells cultured on the prepared biomaterial can be electrically stimulated. The ES mimics the native role of bioelectricity and affects the cellular behavior. The main focus of this review is on the electrical conductivity and stimulation using biocompatible advanced PANI-based materials, documenting and discussing the relevant literature and providing key information and new insights into ES.

1. Introduction

Biomaterial sciences include systematic studies of "engineering" materials with the application purpose in relation with a designated biological system in the human or animals. Comprehensive, exact and predetermined examinations and evaluations are necessary to reach such a specific goal. These examinations are conducted to evaluate the chemical, physical, mechanical and biological properties of biomaterials. A biomaterial can be defined as an engineered material with a specific range of properties, which make it able to stay in contact with

Abbreviations: aECM, artificial extracellular matrix; AFM, atomic force microscopy; ALP, alkaline phosphatase; APS, ammonium persulfate; [BMIM][BF_4], 1-butyl-3-methylimidazolium tetrafluoroborate; [BMIM][NTf_2], 1-butyl-3-methylimidazolium *bis*(trifluoromethylsulfonyl)imide; [BMIM][PF_6], 1-butyl-3-methylimidazolium hexafluorophosphate; BMSCs, bone marrow stromal cells; CHO, Chinese hamster ovary; CNC, computer numerical control; Coll1, collagen type 1; Coll1A1, collagen type 1, α1; CSA, camphorsulfonic acid; CS-G/PANI, chitosan-modified graphene/polyanilie; cTnT, α-actin and cardiac troponin T; CVD-iPSCs, cardiovascular disease-specific induced pluripotent stem cells; DBSA, dodecylbenzenesulfonic acid; DMF, dimethylformamide; DMSO, dimethylsulfoxide; ECM, extracellular matrix; EM, emeraldine base; [EMIM][ES], 1-Ethyl-3-methylimidazolium ethyl sulfate, EmS, emeraldine salt; ES, electrical stimulation; EVAc, ethylene-vinyl acetate; HA, hydroxyapatite; HaCaT, human keratinocyte cells; HEC/PANI, 2-hydroxyethylcellulose/polyaniline; HepG2, human hepatocellular carcinoma cell; hESCs, human embryonic stem cells; [HMIM][FAP], 1-Hexyl-3-methylimidazolium tris (pentafluoroethyl)trifluorophosphate; hMSCs, human mesenchymal stem cells; HOSCs, human osteosarcoma cells; HUVECs, human umbilical vein endothelial cells; IEPs, inherently electroconductive polymers; IFP, interstitial fluid pressure; ITO, indium tin oxide; LM, leucoemeraldine base; NA, nigraniline; NGF, nerve growth factor; NLOs, non-linear optics; NMP, N-methyl-2-pyrrolidone; NSA, naphtalenesulfonic acid; OCN, osteocalcin; OPN, osteopontin; PA, polyacetylene; PABA, poly (aniline-co-benzoic acid); PAMPSA, poly (2-acrylamido-2-methyl-1-propanesulfonic acid); PAN, polyacrylonitrile; PANI, Polyaniline; PANI/PES, polyaniline/ plyethersulfone; PANI-B, PANI base; PANI-Cys, polyaniline-cysteine; PANI-H, HCl doped PANI; PC12, pheochromocytoma 12; PCL, poly-ε-caprolactone; PDMS, polydimethylsiloxane; PE, polyethylene; PEDOT, poly (3, 4-dioxythiophene); PEDs, photo-emitting diodes; PEF, pulsed electrical field; PGLDs, polyglycerol dendrimers; PGS, Poly(glycerol-sebacate); PHBV, poly (3-hydroxybutyrate-*co*-3-hydroxyvalerate); PLA, poly lactic acid; Plexiglas, polymethylmethaacrylate; PLLA/PANI, poly-L-lactide/Polyaniline; PN, pernigraniline base; POSS, poly (styrene sulfonate); PMAP, poly(2-methoxyaniline-5-phosphonic acid); PPy, polypyrrole; PS, polystyrene; PSK, poly (L-lactic acid-co-ε-caprolactone)/silk fibroin; PT, polythiophene; PTFE, polytetraflouroethylene; PTSA, ρ-toluenesulfonic acid; PVA, polyvinyl alcohol; RBCs, red blood cells; RMR, rapid-mixing reaction; RUNX2, runt-related transcription factor 2; SEM, scanning electron microscope; sHya, sulfated hyaluronan; TCP, tissue culture plate; XPS, X-ray photoelectron spectroscopy

* Corresponding author at: Research Center for Pharmaceutical Nanotechnology, Biomedicine Institute, Tabriz University of Medical Sciences, Tabriz, Iran.
E-mail address: yomidi@tbzmed.ac.ir (Y. Omidi).

https://doi.org/10.1016/j.eurpolymj.2018.08.036
Received 29 June 2018; Received in revised form 16 August 2018; Accepted 21 August 2018
Available online 22 August 2018
0014-3057/

the biological systems. Numerous classes of advanced materials such as natural or synthetic polymers can be engineered and used as the biomaterials, including metals, ceramics, composites and hybrid systems. Since the 1970s, there exists an increasing interest in the field of biomaterial sciences. During the past four decades, the number of published scientific documents related to the biomaterials have continuously been increased from 52 documents in 1976 to 4256 documents in 2016 [1]. Such interests in this dominion have indeed resulted in a rapid growth in the global biomaterial market. For instance, this market reached to $ 70.90 billion in 2016 and projected to reach $ 149.17 billion by 2021 [2].

Biomaterial science is a multidisciplinary area of science and technology that include different fields of medicine, biology, physics, chemistry, and engineering [3]. As a simplified definition, a designated biomaterial is the product of the convergence between biosciences and material sciences at the base of engineering.

An early structural definition of the biomaterials is presented by Williams in 1986: “a biomaterial is a nonviable material used in a medical device, intended to interact with biological systems” [4]. On that date, biomaterials were almost completely nonviable materials such as metals and polymers and their application was limited to the medical devices. In consensus with William’s definition of biomaterials, there exist nonviable materials used in medicine, including inert metals such as gold, silver, platinum or commercialized alloys like Stellite® and Vitalium® used in the early designed bone fracture plates; acrylic (methyl methacrylate) polymer used in Judet prosthesis for the femoral neck fracture or commercialized polymers such as Dacron® used in the vascular implants and the heart valves [4,5].

To date, various biomaterials have been developed for the complex systems with viable ingredient(s). Further, various cells [6–9], and bacteria [10,11] have been used in the production of biomaterials. In terms of its applications, in addition to the medical devices, biomaterials have widely been used in regenerative medicine [12–18], pharmacy [19–23], tissue engineering [24–28], biosensors [7,29–34], and some other fields. Thus, we need to expand our views in William‘s definition, perhaps by eliminating the word “nonviable” and the phrase “medical devices”, to get a much broader concept of the biomaterials.

A biomaterial engineered to interact with a biological system should ideally show high biocompatibility while presenting appropriate responses to the biological setting as a measure of biocompatibility in a biomaterial [4]. It seems that the phrase “appropriate response” requires interpretation. Based on the interaction of biomaterials with a biological system, three generations of biomaterials can be recognized, as follows:

(a) The first generation of biomaterials developed during the 1960s and 1970s for the medical devices. These materials engineered for the tissue replacement in the human body with a minimum toxicity. To reach this goal, the first generated biomaterials are almost “inert” in contact with the biological settings. In fact, the inertness has been considered as one of the most common features of this generation. Materials such as platinum, gold, and aforementioned alloys have been used in the replacement prosthesis are common examples of early developed “bioinert” biomaterials [35].
(b) The second generation of biomaterials was introduced in the 1980s, which can be recognized by controlled-reaction with the biological entities. The surface-tissue interactions in this generation play the main role to present the controlled-reaction [36]. The best examples of the second generation of biomaterials (the so-called “bioactive” biomaterials) include bioactive ceramics based on HA or other materials [37–40], bioactive glass-ceramic systems [41–43], bioresorbable materials for surgery and other biomedical applications [44–47] and biodegradable materials with controlled-release of drugs in some pharmaceutical systems [48–55].
(c) The third generation of biomaterials was introduced with certain features such as the potential to mimic the original function of a certain tissue or organ in the human body – the so-called “biomimetic” biomaterials [56]. This generation of biomaterials is generally applied in the tissue engineering and regenerative medicine as the scaffolds. They are 3D matrixes composed of natural or synthetic biodegradable materials supplemented with growth factors, therapeutic agents, peptides and enzymes and even stem cells. They can effectively replace with damaged tissue in the body. In fact, a scaffold forms a platform for the treatment of a damaged tissue by mimicking the natural functions of the cognate tissue.

Taken all, it can be noted that appropriate characteristics of biomaterials in a biological system are “inertness”, “activation” and “mimicry” for the first, second and third generations, respectively. Nevertheless, such categorization can be revisited based on different perspectives; readers are referred to the following studies [57,58].

Of various materials used for the production of biomaterials, the synthetic biocompatible polymers show great physicochemical properties and can be simply produced in a large-scale, including poly (lactic-co-glycolic acid) [59].

Of the synthetic polymers, PANI is a member of IEPs family. Further, PA, PPy, PT, PEDOT, and PANI are the most commonly investigated IEPs. PANI seems to be superior to other IEPs, in large part because of several features, including (a) good thermal stability, (b) cost-effectiveness of the use of aniline as a less expensive monomer, (c) simple synthesis procedure, and (d) good conductivity [60].

PANI-involved complex materials have widespread applications in the electronics, sensors, smart membranes, batteries, optical devices, and biomaterials. This review provides a comprehensive overview about the biological applications of the PANI and discusses its electrical conductivity and biocompatibility.

A sound scientific use of an electroconductive biomaterial such as PANI- involved materials is their applications in the ES process. It should be noted that the bioelectricity imposes inevitable impacts on the functions of the biologic systems, including signaling of the nervous system, muscular contraction and wound healing. Therefore, ES can be used to mimic the original bioelectricity functions in the human body [61].

A rational, scientific and step-by-step program can be considered to (a) synthesize a PANI-involved biomaterial, (b) confirm its electrical conductivity, (c) validate its biocompatibility, and (d) use it as a scaffold with ES effects on cultured cells. Such programs can be expanded towards clinical trials and market. Since there is a lot of information about the synthesis of PANI-involved materials in the literature [62–64], we provide key information about the biological applications of the PANI-involved materials.

In the first section, this review presents some insights into the PANI-based materials applications in different fields. In the second section, we will focus on the electrical conductivity as the main feature of such materials. Parameters affecting the electrical conductivity of the PANI-based materials will be discussed in relation with the ES effect.

2. Polyaniline-based electroconductive materials

A typical polymeric system encompassing PANI as its main component shows great potential to be used in different areas. Applications of such system can be categorized based on the indexed properties of PANI, including electrical conductivity, magnetic activity, thermal sensitivity, optical benefits and specific mechanical features. Of these features, the electrical conductivity seems to be the main feature of the PANI-based systems. We provide comprehensive insights into the electrical conductivity of PANI used as a biomaterial in the next section even though PANI has been used in different fields. The PANI-based composites have widely been used in the production of sensors/biosensors and semiconductors, in large part because of the electroconductive potentials [65–69]. Sensors and biosensors indeed benefit from the PANI-based materials, which can be used for the detection of a

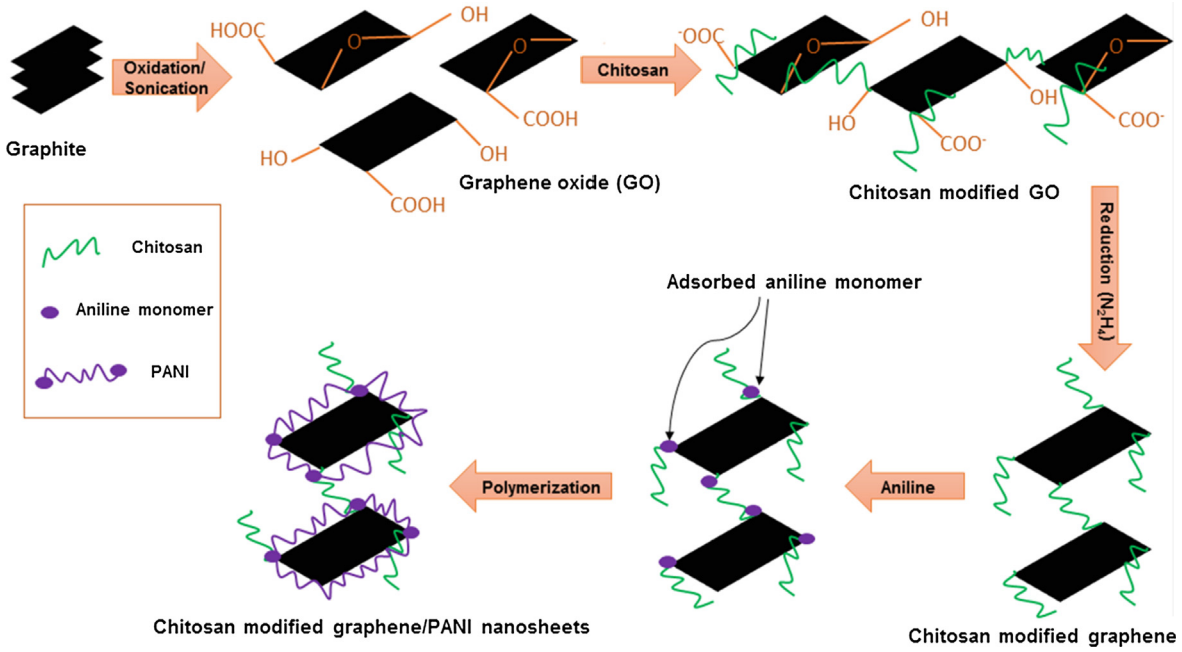

Scheme 1. Synthesis of CS-G/PANI composite as an example of "engineered" material.

Table 1
Main applications of PANI-based materials in different fields (bioscience is not involved).

Main field of PANI based materials application	Main property of PANI	Applications	Ref.
Sensors	Enhancement in electrical conductivity, Signal amplifying	Gas sensors	[70,80–83]
		Glucose sensors	[84–87]
		Sensors for DNA and nucleic acids	[88–91]
		Sensors for biologic and therapeutic agents	[92–94]
Biosensors	Signal amplifying, Potential substitutable platform for enzyme attachment	Glucose biosensors	[95–105]
		Biosensors for DNA and nucleic acids	[106–110]
		Cholesterol biosensors	[111–113]
		Urea Biosensors	[73,74,114,115]
		Biosensors for therapeutic agents and biologic markers	[74,116–121]
		Biosensors for microorganisms	[71,72]
Semiconductors	Variation of oxidation states responding to the electrical current, Variation in conductivity responding to thermal changes	Capacitors and supercapacitors	[75,122–128]
		Memory device	[129,130]
		Solar cells	[131–146]
		Diodes	[147–149]
Photonics	Response to the electromagnetic field or radiation, light emitting in different excitation levels	Nonlinear optics (NLO)	[150,151]
		Organic light emitting diodes (OLEDs)	[152–156]

wide range of analytes from simple molecules like H_2 [70] to even macromolecules and microorganisms [71,72]. A PANI-based material used in the composition of a biosensor usually shows dual functions of an electrical signal amplifier, and a substrate for successful binding of biologic agents (e.g., enzyme) [73,74].

Besides, the PANI-based materials have widely been used for the development of electrodes in capacitors and supercapacitors. For instance, recently, Htut and coworkers introduced biodegradable PANI-based electrodes for supercapacitors [75]. In this work, an environment-friendly approach was established for the synthesis of a CS-G/PANI composite. This composite is an example of engineered materials to achieve a multipurpose system. Scheme 1 shows the synthesis of the composite.

Every component in this composite has its own exclusive role. Graphene is used as the precursor of the composite, and in an acidic medium, it can be oxidized by potassium permanganate yielding carboxyl groups. Chitosan is grafted to the surface of graphene via these groups. The subsequent reduction is then applied to eliminate the unbounded groups of chitosan. Aniline monomers are then adsorbed onto the chitosan bounded sites – a process so-called in-situ polymerization. In fact, this method is a PANI polymerization guided by chitosan that imposes functions of enhancing nucleation growth during the oxidative polymerization and stabilizing by preventing the graphene oxide re-stacking after the reduction process. The dispersion of CS-G/PANI composite in water after one week revealed that chitosan can also improve the stability. The prepared electrode using this composite was found to display markedly higher capacitance ($340\ F\ g^{-1}$) than the G/PANI composite at a current density of $1\ A\ g^{-1}$. After 1000 charge/discharge cycles, the capacitance of electrode was reported as high as 74% of the initial value.

Based on their oxidation states, the PANI can exist in three forms, including (a) reduced form of LM, (b) oxidized form of PN, and (c) the half-oxidized form EM in which the backbone is involved in alternating reduced and oxidized unites [76]. Of these, emeraldine is the most

stable and conductive form of PANI [77].

EM shows a low electrical conductivity in comparison with metals, and therefore it acts as a semiconductor in terms of the electrical conductivity. PANI also responses to the temperature changes, and hence, it is considered as a suitable material for the development of semiconductors. The PANI electron-donating or electron-accepting behaviors can be changed depending on the different oxidation levels. Thus, materials with PANI in their structure used as semiconductors have found their application(s) in the production of memory devices, solar cells, and diodes (Table 1).

It should be noted that the PANI can response to the electromagnetic radiation and although the electromagnetic field in the optical systems. This behavior provides a great basis for applying the PANI-based materials in the development of photonics. Materials with PANI components have also found applications in the NLOs and PEDs. Table 1 lists the main applications of the PANI-based materials in different fields other than the applications in biosciences. It should be considered that Table 1 just presents the main applications of PANI-based materials in simplest categorizations. There are comprehensive review articles with different objectives rather than this review, which introduce other types of PANI-involved materials with most applications in numerous fields of science [78,79].

3. Electrical conductivity in PANI-involved systems

The main focus of this study is on the electrical conductivity of the PANI-based materials, which is the main feature of any IEPs including PANI. In this section, we briefly present an overview of the basic theories related to the electrical conductivity of IEPs, and then discuss different parameters affecting the electrical conductivity in PANI-based polymeric systems.

3.1. Basic concepts in the electrical conductivity of IEPs

The electrical conductivity of PANI, as a member of the IEP family, depends on the inherent structure of the polymer. Backbone in this family of polymers includes a range of monomers with conjugated multiple bonds, which contains a series of an alternating single (σ) and double (π) bonds. Delocalized electrons involved in the extended π network, as well as enduring the strength of the chain by σ bonds make IEPs capable of electrical conductivity as a unique trait of these materials [157,158]. Scheme 2 shows the simplified chemical structure of a conjugated system and the role of different types of bonds in the system.

PANI, in the form of EM, shows a low conductivity at the range of 10^{-1} S cm^{-1}, while it can be converted into the electroconductive EmS

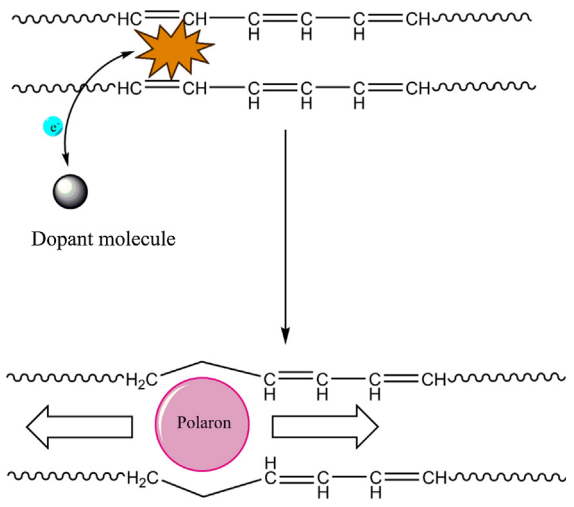

Scheme 2. Simplified mechanism of electrical conducting in IEPs.

form via the process called doping, see Scheme 2 for details [159]. In 1977, Shirakawa et al. reported over 10-fold enhancement in the conductivity by chemical doping using iodine vapor [160]. Doping plays a key role in the conductivity of IEPs. Doping is the process by which a molecule with a localized charge is introduced to the polymer structure and results in the formation of the polaron or bipolaron. As shown in Scheme 2, a polaron in the simplest words is a radical ion associated with a distortion in the lattice [161,162]. Within a potential application, the polaron can travel along the polymer chain, permitting it to conduct the electricity. The polaron movement is achieved by the crystal defects, in which the partially localized electrons in the π bonds favor the formation of polaron while the σ bonds in the backbone of polymer favor the travel of the polaron by enduring the strength of the chain. Similar to semiconductors, doping process can occur when the polymer is oxidized (so-called p-doping) or reduced (so-called n-doping). The doping process is necessary that can be achieved by chemical, electrochemical or photodoping routes [163,164]. Further, details about the physics of electrical conductivity by polarons are reported in a study by Bredas and Street [165].

3.2. Doping and dopant

It has been reported that the magnitude of doping and different type of dopants will affect the properties of the PANI [166–168]. There are several studies reporting a proportional relation between the magnitude of doping and the electroconductivity of PANI [62,169–172]. From the structural point of view, when PANI becomes doped, the polymer changes from the EM form to the EmS form. In these forms, the backbone of PANI includes 50% oxidized units with alternative quinoid and benzenoid rings. Based on these structures, when the doping increases up to 50%, the electrical conductivity of polymer enhances proportionally because in this fraction of doping and a maximum formation of polarons can be achieved. Nonetheless, further increase in doping level results in a decrease in the conductivity. This behavior may be due to the formation of bipolarons with a lower mobility than polarons [62,165,168,170,172,173].

The electroconductivity can be further increased by choosing a suitable type of dopant for doping under optimum condition while this choice can be limited by some changes in other properties of the polymer. The type of dopant and even the doping method can affect the stability, morphology, thermal properties, processability and mechanical properties of a synthesized polymer [174–182].

Acids as routine reagents are used as dopants for the production of electroconductive polymers, in large part because of offering enough protons with a high degree of ionization. Hydrogen protons with high mobility are powerful agents for the electrical conductivity. HCl and different sulfonic acid derivatives are the most popular dopants for PANI. In a number of studies, organic sulfonic acids such as DBSA or PTSA have been used for the doping of PANI because they can improve the solubility and biocompatibility of the polymeric system [183]. Table 2 summarizes some interesting works, in which PANI-based polymeric systems are applied or show potential as biomaterials.

The successful synthesis of a novel flexible electroconductive membrane has recently been reported by Hu et al. In this work, PANI/bacterial cellulose composite was synthesized using bacterial cellulose as a template. The electrical conductivity of composite was found to be influenced by the type of dopant(s) used. The effect of dopant type was investigated using different acids. As a result, it was reported that the composite doped by HCl, H_2SO_4, toluenesulfonic acid, DBSA, phosphoric acid and ammonium sulfonic acid (NH_4SO_3H), while the related conductivities were calculated. A distinct difference between the conductivity of composite was reported when HCl was used as a dopant ($\sigma \approx 0.05$ S cm^{-1}) or in the case of other dopants ($\sigma \approx 0.01$ S cm^{-1}) [192].

Although HCl and different sulfonic acids are the most preferred dopants for the PANI-based polymeric systems for the production of

Table 2
Detailed list of recent indexed works in the field of PANI-based biomaterials.

Polymeric system	Maximum electrical conductivity (S cm^{-1})	*In vitro* biocompatibility study	*In-vivo* biocompatibility study	Electrical stimulation paradigm	Ref.
Poly(ethylene oxide) grafted to the PANI surface	–	Adsorbed amount of bovine serum albumin and human blood plasma platelet	–	–	[184]
PANI	–	Adhesion and proliferation H9c2 cardiac rat myoblast cells	–	–	[185]
Electrospun PANI and gelatine	2.1×10^{-2}	Cell viability of H9c2, cardiac rat myoblast cells	–	–	[186]
PANI	1.0	Proliferation and adhesion of PC-12 pheochromocytoma cells	–	–	[187]
Electrospun PANI and poly(l-Lactide-co-ε-caprolactone)	1.4×10^{-2}	Cell viability of human dermal fibroblast, NIH-3T3 fibroblast, and C2C12 myoblast cells	–		[188]
PANI-collagen composite	–	Cell viability of Porcine skeletal muscle cells	–	–	[189]
PANI	–	Proliferation and adhesion of PC-12 pheochromocytoma cells	–	–	[190]
Electrospun nanofibers of poly(lactic acid) blends with PANI or poly(aniline-co-benzoic acid)	2.0×10^{-2}	–	–	–	[183]
Electrospun poly(aniline-co-3-aminobenzoic acid) (3ABAPANI) and PLA blends	8.0×10^{-3}	Cell viability of African Green Monkey fibroblast COS-1	–	–	[191]
PANI-Bacterial cellulose nanocomposite	1.0×10^{-2}	–	–	–	[192]
Electrospun dendronized PGLD-PANI nanotubes	–	Cytotoxicity study using CHO cells; Cardiac regeneration study using cardiac myocytes of rat	–	–	[193]
PANI-PGS copolymer	1.77×10^{-2}	Cell viability, adhesion, and proliferation of C2C12 myoblast cells	–	–	[194]
Electrospun PANI-PLLA nanofibers	3.0×10^{-9}	Adhesion and proliferation of rat nerve stem cells (C 17.2)	–	100 mV mm^{-1} for 60 min	[195]
PANI	2.5×10^{-4}	–	–	–	[196]
PANI	–	–	Acute toxicity and teratogenic assay using *Rhinella arenarum* (common South American toad) larvae	–	[197]
PANI	–	Cell viability of human immortalized HaCaT, HepG2	Sensitization experiments performed using 25 non-pregnant healthy female of Dunkin-Hartley guinea pigs Skin irritation tests performed on 30 healthy individuals (20 women and 10 men).	–	[198]
Electrospun PANI-PLGA nanofibers	–	Cell viability and immunofluorescence study using Rat neonatal cardiomyocytes	–	Electrical pulses of 1.25 Hz and 5 V cm^{-1}	[199]
PANI	140	Cell viability of NIH/3T3 fibroblast	–	–	[200]
PANI	10	Cell viability, apoptosis detection, ROS detection, immunocytochemistry study and RTPCR study of hMSCs	–	Electrical pulses of 100 mV cm^{-1} for 10 min day^{-1} and for 7 days	[201]
Electrospun nanofibers of PANI and PCL	2.0×10^{-4}	Cell viability of L929 murine fibroblast cells	–	–	[202]
Polyacrylonitrile – Polyaniline composite nanofiber webs	2.0×10^{-2}	–	–	–	[203]
PANI	–	Blood coagulation and platelet adhesion study	–	–	[204]
PANI	–	Cell viability, gene expression analysis, cytotoxicity study and calcium detection for bone marrow-derived hMSCs	–	Rectangular electrical pulses (6 ms, 3.6 mV cm^{-1}, 10 Hz) for 4 h followed by 4 h break for 28 days	[205]
Cysteine modified PANI supported onto PET films	–	Cell viability of human immortalized HaCaT and mouse lymphoblasts (LM2)	–	–	[206]
Nanostructured PANI on ITO glass	–	Cell proliferation of PC-12 cells; Dynamic protein adsorption analysis using the SDS-PAGE technique	–	Rectangular pulses (100 μA, 0.8 ms) repeating every 1 s for 1, 2 and 4 h	[90]

(*continued on next page*)

Table 2 (*continued*)

Polymeric system	Maximum electrical conductivity (S cm^{-1})	*In vitro* biocompatibility study	*In-vivo* biocompatibility study	Electrical stimulation paradigm	Ref.
PANI-conjugated PHBV	5.8×10^{-5}	Cell viability and cell cycle analysis using NIH/3T3 fibroblast hemolytic assay Wound healing assay Protein adsorption study	–	–	[207]
HEC/PANI nanocomposite	10.0	Cell viability and actin fluorescent imaging of l929 mouse fibroblasts	–	2.5 V cm^{-1} and 2 mA for 24 h	[208]
PANI-coated PCL fibers	6.7×10^{-3}	Cell viability of HUVECs	–	200, 300 and 400 mV cm^{-1} 30 min day^{-1} for 4 days	[209]
PANI/polyethersulfone (PES) nanofibers		Cell viability, RT-PCR study, karyotyping study and immunofluorescence staining of CVD-iPSCs	–	Electrical pulses for 1 h day^{-1} for 15 days	[210]

biomaterials, the PANI-based electroconductive polymers have so far been doped using macromolecules, including polymeric acids, ionic liquids, and aforementioned agents (mostly in other fields). For example, Wei et al. doped PANI with the star-like POSS. First, polystyrene-tethered POSS (POSS-PS) core was synthesized by coupling reaction between POSS-CL substitute and anionic living PS chain. Next, sulfonated POSS-PS core was synthesized via Makowski's method, in which acetyl sulfate was used as sulfonation reagent. Finally, having utilized oxidative polymerization, where APS used as the oxidant, PANI was doped with a synthesized dopant. Scheme 3 illustrates the synthesis route and chemical structure of applied reagents. The exclusively developed dopant used as a flexible template to let PANI chains, continue to grow along with the chains of the dopant. Using such a template, PANI with loose packing structure has been prepared [211].

Recently, Qu and Zeng successfully applied ionic liquid as a dopant for the electrochemically synthesized PANI on a glassy carbon electrode. They studied five different 1-alkyl-3-methylimidazolium-based ionic liquids, including [BMIM][BF_4], [BMIM][NTf_2], [BMIM][PF_6], [EMIM][ES] and [HMIM][FAP]. Such studies were conducted considering different combinations of anions and cations as electrolytes/dopants. They showed that ionic liquids are the most capable dopants for the electrochemically synthesized PANI, concluding that doping PANI with such dopants offers many opportunities to develop more versatile materials [212].

The type of dopant reagent can also impose its effect on other characteristics in a synthesized polymeric system. For example, the effect of the type of dopant on the morphology of prepared systems was studied.

Using oxidative dispersion polymerization, Bhadra et al. synthesized PANI/ PVA blends doped with HCl [213]. To produce EmS, a dedopping was performed by introducing to NH_4OH solution and stirring for 3 h. The system was then redoped with CSA, NSA, PTSA, and DBSA. Having applied this strategy, they were able to investigate the effect of using different sulfonic acids as a dopant on the electrical conductivity, thermal stability, and morphology of blends. A slight effect on the conductivity was then reported. The minimum electrical conductivity was attained using NSA as a dopant (4.4×10^{-3} S cm^{-1}), while the maximum electrical conductivity was achieved using DBSA as a dopant (6.2×10^{-2} S cm^{-1}). It was found that the morphology of blends was markedly affected by the type of dopant. Having used such approach, different morphologies with different particle sizes and shapes have been obtained using NSA, CSA, PTSA, and DBSA, including nanospheres 200–240 nm), nanospheres (70–90 nm), hexagonal nanoflakes (60–100 nm) and nanorods (diameter 50–70 nm and length 200–500 nm), respectively. In this line, Ravi Kumar et al. compared HCl and DBSA as dopants and their effects on the conductivity and morphology, reporting similar results, as shown in Fig. 1 [214].

3.3. Composition of polymer

The composition of polymer plays a key role in the electrical conductivity of a system. Abdul Rahman et al. investigated the influence of polymer composition on the conductivity of electrospun PLA blend with PANI or PABA. The changes in the absorbance (273 nm) was analyzed to estimate the composition of the copolymers with different mass ratios of PANI or PABA used in the structure. A proportional increase in the conductivity of copolymers was reported with an increase of the mass percentage of PANI or PABA. When the amount of PANI in the composition increased from 0% to 3.27%, a significant increase (i.e., from 3.9×10^{-9} mS cm^{-1} to 2.0×10^{-5} mS cm^{-1}) in the conductivity was recorded. The same behavior was reported in the case of PABA. Increase in the amount of PABA in the composition from 0% to 5.80% causes an increase in the conductivity from 3.9×10^{-9} to 8.3×10^{-6} (mS cm^{-1}). Comparing PANI with PABA, a logical pattern can be deduced in terms of the relation between the conductivity and the composition of different polymeric systems. Generally, it can be

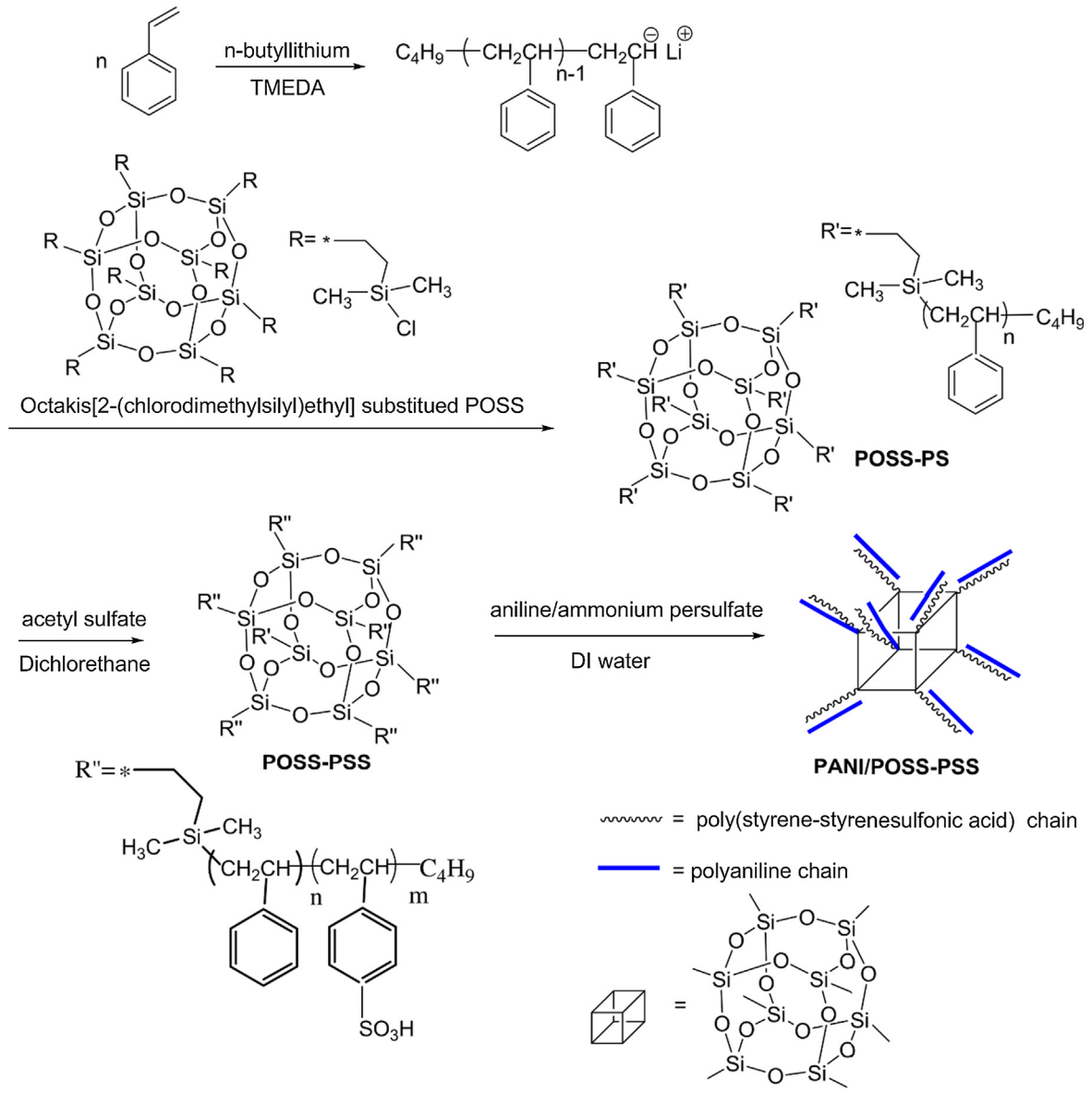

Scheme 3. Synthesis rout of star-like poly (styrene sulfonate) doped PANI. Role of an exclusive dopant in the polymerization. Reproduced with permission from Ref. [211]. Copyright 2012, Elsevier.

conceptualized that the higher the mass ratio of PANI in the composition of a system is, the greater the electrical conductivity will be. As result, it can be inferred that pure PANI can provide a higher conductivity than its derivatives [183].

In a remarkable work, the electrical conductivity change in PANI-PGS copolymers with different composition was studied for 4 days. PANI content in these copolymers differed from 15% to 30%. Their conductivity was compared to the pure PGS. Following the above-mentioned concept, the electrical conductivity of the polymers improved from 1.29×10^{-3} S cm^{-1} to 1.77×10^{-2} S cm^{-1} by increasing the content of PANI from 15% to 30%. The obtained results in this work showed that the conductivity of the copolymers reduced with the time to some extent but not below the order of magnitude for any of the composite samples over 4 days. For example, the conductivity of copolymer with 30% of PANI content, decreased to 1.03×10^{-3} S cm^{-1} after 4 days [194].

3.4. Synthetic parameters

The electrical conductivity can be affected by the synthesis condition and rout. A PANI-based material routinely synthesized through an oxidative polymerization approach in the presence of an acidic dopant agent. In such an approach, aniline monomer usually was dissolved in an aqueous solution of dopant. Then, the polymerization was occurred by adding a calculated amount of an oxidant such as APS, or a calculated volume of its solution to the reaction medium. The prepared polymer might be converted to a dedoped form by treating with a weak base solution (e.g., ammonia solution). Many parameters seem to affect the properties of the synthesized material, including the concentration of applied solutions and their proportion to each other, the type of dopant and/or oxidant agent and other physical variables such as temperature.

Decreased solubility is a challenge in PANI-based materials. When the polymerization reaction begins with a functionalized PANI such as PMAP, a self-doped electroconductive PANI-based material is achieved, in which the dopant agent is bonded to the backbone of PANI as a functional group. The self-doped PANI-based materials show an improved solubility in different organic solvents [215].

In a notable study, Blinova et al investigated the conductivity of PANI synthesized using a solution-gelatin interface. Researchers have

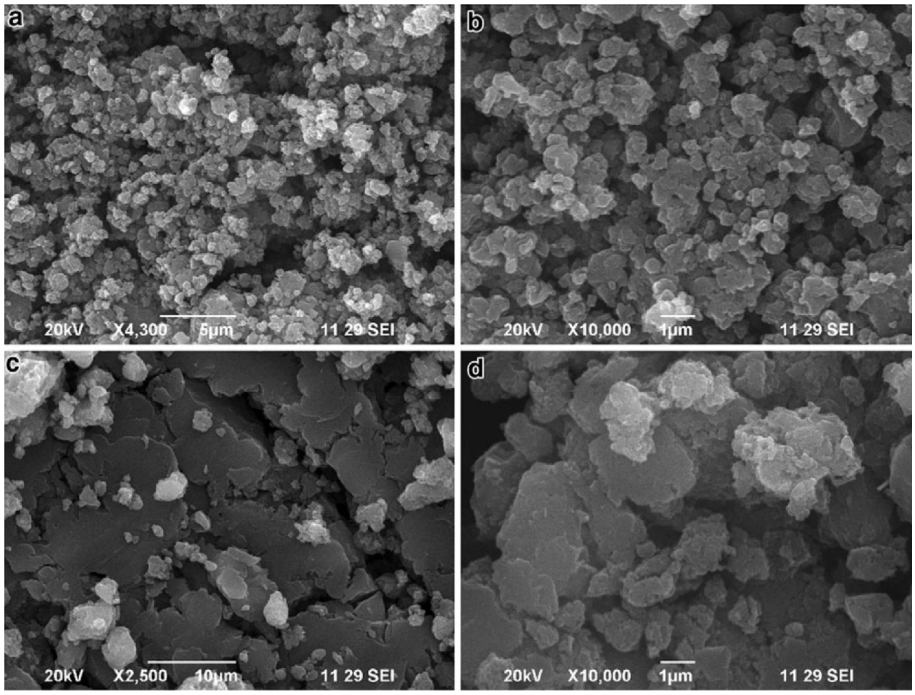

Fig. 1. Effect of dopant type on the morphology of doped polymer. Poly (aniline-*co*-*m*-aminoacetophenone) doped with DBSA (a,b) and HCl (c,d). Reproduced with permission from Ref. [214]. Copyright 2013, Springer Nature.

synthesized PANI in two different conditions and compared the conductivity, including the condition (a) where the aniline hydrochloride traffics from the gelatin while the APS dissolves in the solution, and the condition (b) where the APS traffics from the gelatin and aniline hydrochloride from the solution. Oxidant to aniline mole ratio was 1–25 in two conditions. The maximum conductivity was reported under the condition b when the PANI fraction was grown at the surface of the gel (up to 7.2 S cm^{1}) and the aniline fraction was produced inside the gel conductivity (up to 1.9 S cm^{-1}). Having used the same concentration of aniline (i.e., 0.2 mol L^{-1}) and under the condition a, the electrical conductivity was reported to be 0.23 S cm^{-1}. Altogether, based on the synthesis conditions used, an overall 35-time increase in the conductivity of the system was reported [216].

Ucar et al. examined the effect of different synthetic parameters on the conductivity, morphology, thermal stability, crystallinity and tensile properties of CSA doped polyacrylonitrile/PANI (PAN/PANI) composites. In this work, an oxidative polymerization was carried out using DMF, DMSO, NMP and their mixtures. The concentration of PANI in all solutions was kept constant (10% w/w). The conductivity of composite produced using DMSO/DMF mixture was reported to be about the same level of that of the nanofibers produced using DMSO (i.e., 1.88×10^{-6} S cm^{-1} for the DMSO/DMF mixture and 4.82×10^{-6} for the DMSO. Further, the conductivity of nanofibers produced using NMP and NMP/DMF mixture were compared. The nanofibers produced using solvent mixture showed almost 10^{3} times improvement in the conductivity values (i.e., 4.63×10^{-9} S cm^{-1} for NMP and 2.97×10^{-6} NMP/DMF mixture). This improvement in the electrical conductivity appears to be associated with the better dissolving of PANI in NMP and the presence of DMF. Besides, about 10time additional increase in the conductivity of nanofibers (from 4.82×10^{-6} to 1.74×10^{-5} S cm^{-1}) was reported after two times redoping. The conductivity was not affected by the further redoping and mechanical dispersion processes [203]. A similar comparison between PAMPSA doped PANI and PTSA doped PANI nanofibers was reported by Zhang et al. Further, the effect of different synthesis parameters such as reaction time, interface area (in interfacial polymerization), reactant concentration and reaction value were investigated. These parameters were found to have a deep effect on the morphology with a moderate effect on the conductivity [196].

Taken all, the electrical conductivity of PANI-based materials can be influenced by a wide range of parameters. To get the desired PANI-based materials, one needs to establish an optimal balance between the electrical conductivity and other properties.

4. PANI-based materials: the challenge of biocompatibility

The electrical conductivity and biocompatibility of PANI are the two key features that need to be considered for a successful development of an electroconductive biomaterial. Validation of the biocompatibility appears to be much more challenging than the electrical conductivity, in large part because of dealing with a biological setting *in vitro* and/or *in vivo*. Thus, the biocompatibility characteristics are discussed in details in the following sections.

4.1. Biocompatibility: what does it mean?

Park and Lakes described the word “biocompatibility” in their textbook as follows: “the acceptance of an artificial implant by the surrounding tissue and by the body as a whole. The biomaterial must not be degraded by the body environment, and its presence must not harm tissues, organs, or systems. If the biomaterial designed to be degraded, then the products of degradation should not be harmful to the tissue”. In practice, the biocompatibility of a designated biomaterial needs to be established and approved by different experimental-analytical methods *in vitro* and *in vivo* in contact with cells, tissue and/or the whole body. The methods applied for the validation of biomaterials must be able to examine a wide range of properties, including mechanical, chemical, pharmacological properties [5].

Biocompatibility studies are routinely conducted in research laboratories and industries. These studies must be executed following specified protocols and under compliance with the certain standards, most of which have been approved by appropriate agencies such as the United States FDA and similar organizations in other countries [217,218].

There are a few simple methods that their results can be reported as an index for the biocompatibility, which does not need to be performed in contact with the biologic medium or components. These methods usually measure the physicochemical properties such as hydrophilicity of polymeric system. The dispersion of the synthesized polymer in the aqueous phase [75,219], and the decrease in contact angle [184,191,202], epitomize two simple methods that measure the hydrophilicity of synthetic materials. The contact angle of a solution of the polymer can simply be performed by a monocular optical microscope [220]. In fact, the hydrophilicity evaluating experiments can provide a scientific prediction for the biocompatibility. Nevertheless, an exact and real determination of biocompatibility needs to be done through specific *in vitro* and *in vivo* tests in the real biologic medium.

4.2. In vitro tests

In vitro tests provide several advantages, including cost- and time-effectiveness, optimized laboratory facilities, simply required equipment and relatively fast processing of large numbers of biomaterials. Cell culture techniques have widely been used to establish *in vitro* tests for the effective screening of the biocompatibility. To evaluate the biocompatibility of a typical biomaterial, some cell functions can be monitored, including adhesion, proliferation, migration, signal transduction, metabolism, biosynthesis, and deposition of extracellular chemical compounds. Mammalian cells of specific tissue/organ can be used for this manner. For instance, cells interacting with electricity such as nerve and cardiac cells are the most probable candidates for testing the electrical conductivity of conductive polymers such as PANI- based polymeric systems [217].

Bidez et al. evaluated *in vitro* biocompatibility of PANI films using cultured H9c2 rat myoblast cells. The nonconductive form of PANI was doped with 1 M HCl to form a conductive emeraldine (E-PANI) polymer. Cell attachment and proliferation up to 200 h on both forms of PANI were investigated and compared with those on the TCP. The H9c2 rat myoblasts attached within 15 min on both conductive and nonconductive forms of PANI. The H9c2 cells grown on the E-PANI showed a slightly prolonged lag phase, perhaps because of the presence of somewhat residual acid dopant. For the same reason, doubling times for the cells grown on the E-PANI were slightly prolonged as compared to the TCP control. Notably, after approximately 100 h of seeding on the E-PANI, the cells were rapidly proliferated and reached a plateau similar to the cells on the TCP control [185].

Wang et al reported the cell compatibility of nanostructural polyaniline films doped with different acids. In this study, the synthesized PANI was doped with perchloric, hydrochloric, malic and citric acid during polymerization. The films were then subjected to the electrical conductivity and surface roughness examinations as wells as cell biocompatibility tests. To evaluate the *in vitro* biocompatibility of polymers, the PC-12 pheochromocytoma cells were used and their adhesion, spreading and proliferation were studied. The cell adhesion 1 h after the seeding was significantly enhanced on the synthesized PANI film surface as compared to the casting PANI. Only about 30% of cells attached to the casting PANI, while the cell attachment on the other surfaces was much higher (up to 70%). Further, the cell proliferation using the synthesized PANI films, casting PANI and PTFE were investigated. The synthesized PANI films, composed of nanoparticles 30–50 nm in size, provided much better results in the terms of the cell attachment and proliferation in comparison with the casting PANI. Initial proliferation (1-day post-seeding) was found to be faster for the malic-doped MA-PANI and the citric acid-doped C-PANI than for the PTFE ($p < 0.05$). After 2 days of the cultivation, an increase in DNA in the HCl-doped H-PANI, and casting PANI were recorded as compared to the PTFE. Finally, on the fourth day of the seeding, the DNA content in each group was quickly increased. Fig. 2 shows the cell biocompatibility of PANI doped with different acids [187].

In another work, using PC-12 cells derived from the pheochromocytoma of the rat adrenal medulla, Liu et al. investigated the *in vitro* biocompatibility of PANI film. They looked at the proliferation behavior and survival of this cell line seeded on the PANI film, bare Si substrate, and 24-well TCP plates. The cells were allowed to proliferate on different substrates for 4 days. After 1 day of the cultivation, the number of PC-12 cells on the PANI film was significantly larger than that of the Si bare surface. After 2 days of the cultivation, the cells continued to proliferate on the PANI film but not on the Si wafer. The survival rate of PC-12 cells cultured on the TCP plates on the initial 2 days was much higher than that of the PANI film and the bare Si film. With prolonging the culture time to 4 days, the survival rate of cells cultivated on the PANI film was the highest among the tested substrates [190].

Moura and de Queiroz developed dendronized PANI nanotubes for the cardiac tissue engineering. First, they synthesized PGLDs with an average molecular weight of 1.7 kDa and about 26 hydroxyls per molecule in a step-growth process denominated divergent synthesis. Then, to improve the biocompatibility of PANI, the synthesized PGLD was immobilized on the surface of PANI nanotubes by a ring-opening reaction of epoxy on PGLD. In this work, the cytotoxicity of electrospun PGLD-PANI nanotubes was evaluated by an *in vitro* test using CHO cells. The biocompatibility of polymeric system was evaluated *in vitro* in the cardiac myocytes primary cell culture isolated from the ventricular portion of hearts of 2- to 4-day-old Sprague-Dawley rats. This study revealed that PGLD-PANI nanotubes formed electrospun fibers could promote the proliferation and differentiation of myocardial cells with no/trivial toxicity [193].

In a detailed study, Humpolicek et al. evaluated the biocompatibility of PANI *in vitro* and *in vivo*. The main focus of this study was on the PANI powder's cytotoxicity, irritation, and sensitization. *In vitro* tests were performed using the human immortalized HaCaT in a pilot study and the HepG2 in the second extended study. This study showed that the cytotoxicity of PANI can deeply be affected by the reprotonation of PANI base to produce the RD-PANI-B, and subsequence deprotonating. PANI-B itself was prepared by immersing primly synthesized PANI-H into the large excess of 1 M ammonium hydroxide. Generally, the lower concentration of the extract caused a lower cytotoxicity in different cell lines. The HaCaT cells cultivated with PANI-H in a concentration higher than 25% m/v showed a severe cytotoxicity with cell survival below 40%, while in the case of HepG2 cells none of the tested extracts displayed such cytotoxicity. While the concentration of PANI-H was reduced down to 1% to obtain a non-cytotoxic system for the HaCaT cells, 10% PANI-B extract did not show any toxicity. In the case of HepG2 cell line, similar reduced cytotoxicity levels were observed using 25% of PANI-B and 5% of PANI-H extracts. The use of HCl during polymerization and the presence of chloride counter-ions, which can negatively affect the cell viability, seem to be the probable reason(s) for the biocompatibility differences between the samples [198].

Mouse embryonic fibroblast NIH/3T3 cells were applied for *in vitro* biocompatibility testing of PANI by Stejskal and coworkers [200]. Nanoscale PANI with globular and tubular morphology was prepared by the oxidative polymerization as well as using HCL and acetic acid as the dopant. Samples were purified from two different solvents, NMP and concentrated sulfuric acid in methanol. Cytotoxicity studies were carried out after 24 h after the seeding by MTT assay and then the absorbance was measured at 270 nm. The cytotoxicity of purified polymers investigated in compliance with the ISO 10993, in which the cells treated with polymer's extractions with different concentrations. The cytotoxicity of different PANI salts precipitated from acidic solutions were compared with each other. Globular samples processed from the NMP displayed higher cytotoxicity of the extracts (5%) than that of the extracts obtained from the nanotubular sample (10%). Furthermore, in the case of samples dissolved in sulphuric acid instead of NMP, a significantly decreased cytotoxicity was reported for 100% and 50% of the extracts. This effect was observed for both globular and nanotubular samples. The researchers articulated some possible reasons for such a

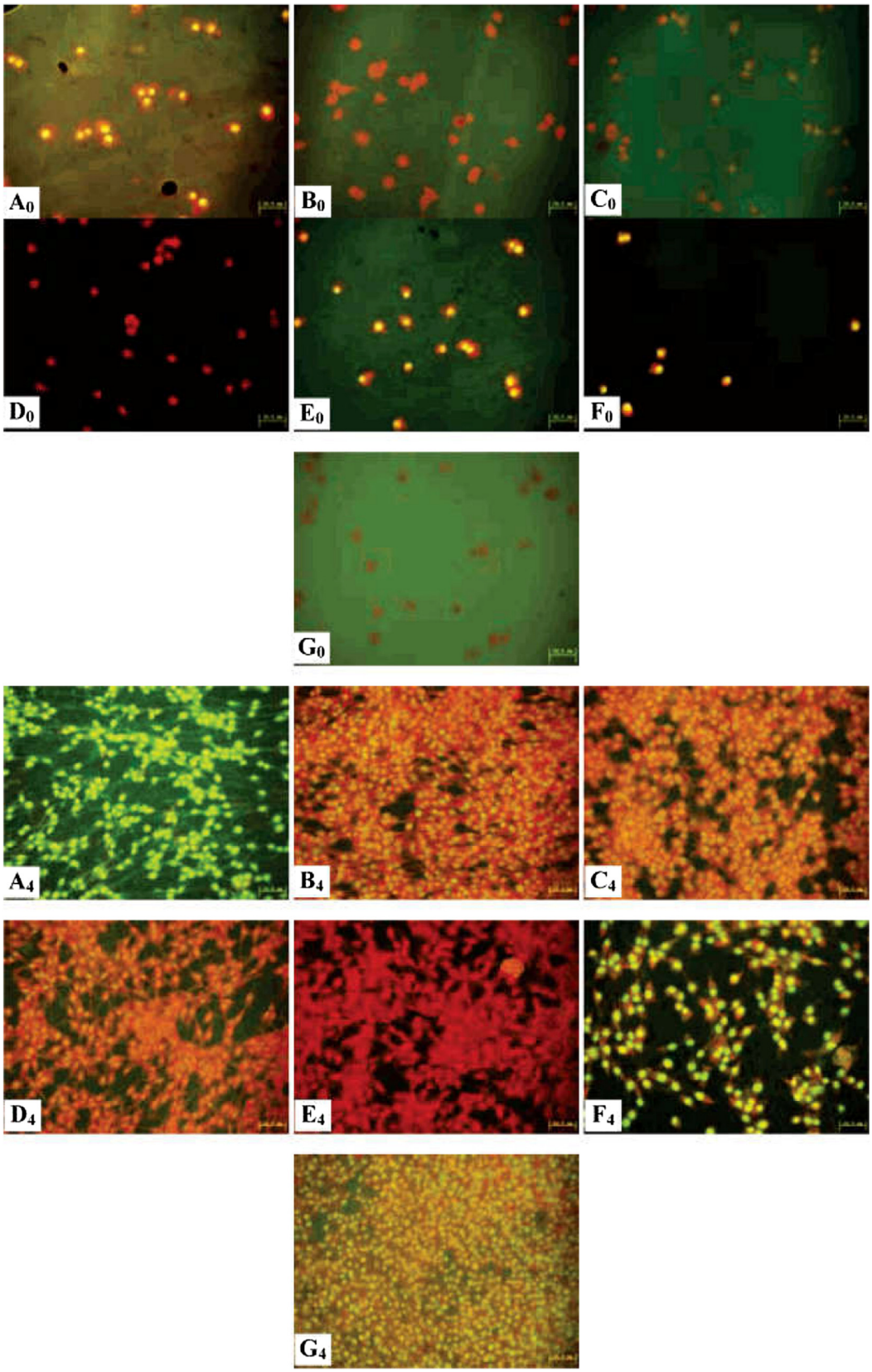

Fig. 2. Effect of dopant type on the biocompatibility of the polymer. Biocompatibility was tested in the PC-12 pheochromocytoma cells cultured on PTFE (A0-A4), PANI doped with perchloric acid (B0-B4), hydrochloric acid (C0-C4), maleic acid (D0-D4), citric acid (E0-E4), casting PANI film (F0-F4), and the plate (G0-G4) for 0 days (A0-G0) and 4 days (A4-G4). All scale bars represent 39.9 μm. Reproduced with permission from Ref. [187]. Copyright 2008, American Chemical Society.

phenomenon [200], yet much more comprehensive researches are required to fully address the issue.

HCl-doped nanofibrous PANI (nfPANI) prepared using RMR method and then different amounts of nfPANI electrospun with PCL to obtain PANI/PCL fiber-scaffolds by Wu and coworkers. The cytotoxicity of prepaid scaffolds was investigated using L929 murine fibroblast cells as a well-established cell line with a high sensitivity to toxins. The cell adhesion and proliferation were analyzed using a resazurin fluorescence assay after 1 and 4 days of seeding. This study clarified the importance of the fiber diameter in terms of the biocompatibility of fiber scaffolds. Compared to the TCP control, larger fibers (6–7 ìm) showed a reduction in the adhesion of 30%-40% of cells, while fibers with an average diameter of 150 nm did not influence the growth of the cells [202].

A biocompatible substrate for the cell culture developed by Yslas and coworkers. They synthesized PANI supported onto the PET films and modified its surface by L-cysteine to improve the biocompatibility of the system. Adhesion and proliferation of the HaCaT and mouse lymphoblasts (LM2) cells on PANI and PANI-Cys substrates were compared to the TCP control after 24 and 36 h seeding. The attachment behavior of both cell lines was studied by the immune fluorescence and further evaluated by morphology analysis using the AFM technique. The number of cells attached to the PANI-Cys and the density of viable cells was interpreted significantly after 36 h of seeding. The AFM analysis of the post-culture showed that the morphology of both cell lines seeded on the PANI-Cys substrate was comparable to each other and to the cells seeded on the TCP control. Authors have inferred that this behavior cannot be overgeneralized to other cell lines [206]. Although the cell culture approach is the most preferred technique to approve the *in vitro* biocompatibility of PANI based biomaterials, some other specific approaches can be recruited for the evaluation of biocompatibility.

Humpolicek and coworkers studied the surfaces of blood collection tubes-coated with either the conductive PANI hydrochloride deprotonated non-conductive PANI, or the PAMPSA reprotonated PANI. Then, they investigated the hemocompatibility of prepared PANI-based polymers. In this research, venous blood was collected from the healthy donors into the tubes. Blood plasma coagulation and platelet adhesion were studied to validate the hemocompatibility of the polymers. The PAMPSA reprotonated PANI exhibited a significant impact on the blood coagulation. This was correlated to the interaction between the polymer and three coagulation factors, Xa, Va, and IIa. The modified-film was reported to display significantly reduced platelet adhesion potential as compared to the standard PANI film or the uncoated reference surface. Protonation of PANI with the PAMPSA shifts the polymer to the biological pH and makes it conductive. Such shifting occurred for the unmodified PANI below the pH 4, while it was seen for the PAMPSA-redoped PANI at the pH 4–6. The reprotonating of PANI with the PAMPSA, in fact, could improve its pH stability, enabling it to be used in the biological pH range. The anticoagulation activity, reduced platelet adhesion in combination with the improved pH stability show a good potential for the use of this modified polymer as a biomaterial [204].

The blood biocompatibility of PANI-conjugated PHBV electroconductive porous scaffolds was studied by Paramanik et al. In this study, a hemolytic assay was established for the curcumin-loaded PHBV-*g*-PANI composite. Saline solution and distilled water used as the negative and positive controls, respectively.

Extreme hemocompatibility reported for the composite, where no inhibition of the RBCs was detected in the contact with the extraction of biomaterial (up to 4 mg mL^{-1}). In the presence of biomaterial (6 mg mL^{-1}), after the incubation for 10 and 120 min, respectively 3.9% and 4.2% of lymphocyte cells were found to be lysed (see Fig. 3). The cell biocompatibility of the PANI/PHBV composite approved using NIH3T3 fibroblasts like to other above-mentioned works. This study is a comprehensive research, in which several features of the developed biomaterial were studied, including *in vitro* wound healing, surface adsorption of protein molecules, antimicrobial activity upon gram-negative and gram-positive microorganisms and electrical conductivity [207].

4.3. *In vivo* tests

These tests use the animal models to evaluate the biocompatibility of biomaterials. Further, such experiments can be developed toward clinical trials in the human subjects. Once approved, they can finally reach the market. The use of laboratory animals demands certain ethical issues and approval after successful completion of premier material analyses and *in vitro* tests [217]. Different examinations need to be implemented for the evaluation of *in vivo* biocompatibility of biomaterials. A list of such experiments includes the following steps: sensitization, irritation, intracutaneous reactivity, systemic toxicity, subchronic toxicity, genotoxicity, implantation, hemocompatibility, chronic toxicity, carcinogenicity, and biodegradation [218].

In a pioneering work, *in vivo* tissue response to PANI have been studied by Wang et al. Different forms of PANI were implanted in male Sprague Dawley rats. After 24 weeks, the EM film was encapsulated by fibrous tissue. The minimum inflammation associated with the different forms of PANI was reported after 50 weeks [221].

In another work, Kamalesh et al. investigated *in vivo* biocompatibility of PANI in three different oxidative states, EVAc and PE by subcutaneous implantation into Sprague Dawley rats beneath the dorsal skin for 19 to 90 weeks. Since the neoplastic tissues exhibited greater IFP than the normal tissues, IFP analysis was applied to evaluate the extent of biocompatibility before and after the implantation. The surface of the polymers before and after the implantation was studied using XPS. EVAc showed a high-degree of biocompatibility in the rabbit cornea, and hence, was used as the reference for other polymer types. PANI in form of NA, LM, and EM implanted into the rats did not induce a high oncotic IFP for almost two years after the implantation. This fact confirms the absence of neoplastic tissues formation during the period. Furthermore, the histological pictures confirm the biocompatibility of these types of polymers at least in the dorsal region of the skin [222].

Humpolicek et al. performed sensitization experiments using 25 non-pregnant healthy females of Dunkin-Hartley guinea pigs and the skin irritation tests on 30 healthy individuals (20 women and 10 men). Based on the obtained results, the sensitization of PANI was graded as “zero” since none of the tested animals demonstrated erythema and/or edema. In the positive control group, 8 of 30 volunteers showed weak, positive skin reaction. The skin irritation characterized by a mild erythema and/or dryness immediately after the *in vivo* patch soaked with the positive control was removed. About, 24 h after patch removal, the number of the volunteers with positive skin reaction was increased to 27 cases. PANI-H and PANI-B were introduced as the polymers with exceptional biocompatibility properties in terms of the dermal irritation and sensitization tests [198].

Yslas et al. studied the acute toxicity and teratogenic effect of PANI nanofibers on *Rhinella arenarum* (South American common toad) embryos. The acute toxicity test was performed on the pre-metamorphosis (stage 25) larvae, while the teratogenic test, which evaluates the early life stage toxicity, was performed on 2–4 blastomeres stage. Larvae were exposed to PANI nanofibers with the concentration equal to 150, 250 and 400 mg L^{-1} within 96 h. Embryos were fed with PANI as the only available carbon source in the test groups and obtained results as compared to the control group, where the embryos were fed with the fish food. Based on the results, PANI nanofibers exhibited no toxicologic effects in *Rhinella arenarum* larvae were exposed to even the concentration of 400 mg L^{-1} at the 25th stage. However, in the case of developing larvae, PANI nanofibers with the concentration of 250 mg L^{-1} and 400 mg L^{-1} induced a growth inhibition. Fig. 4 clearly shows this teratogenic effect in the embryos. These results showed that the toxicity of the PANI nanofibers to aquatic species might be dependent on the concentration of the PANI and could have been deeper in

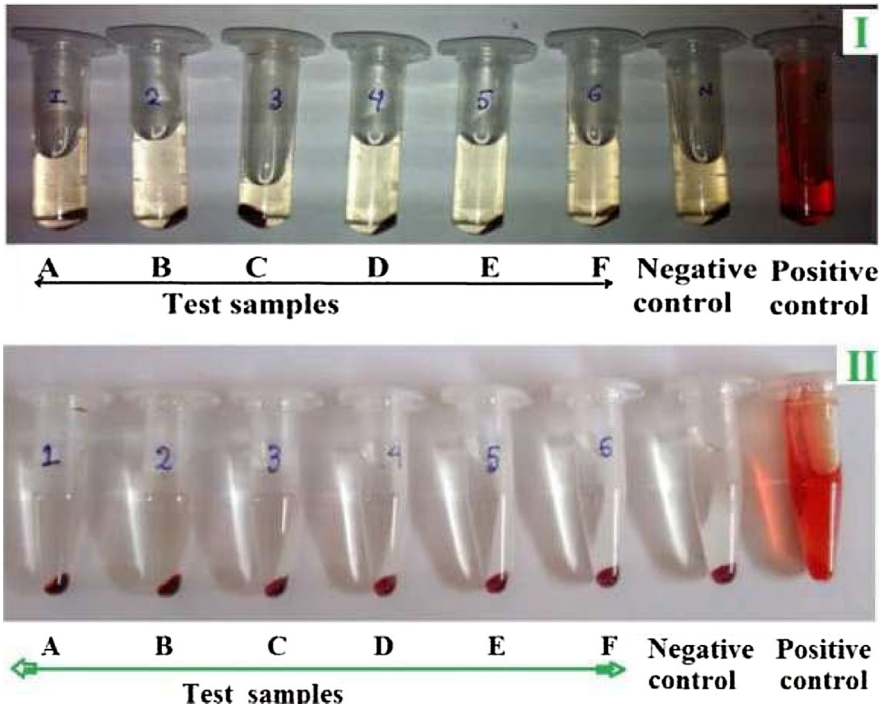

Fig. 3. Blood biocompatibility assays of curcumin-loaded PHBV-*g*-PANI composite-based films: (A) 1 mg mL^{-1}, (B) 2 mg mL^{-1}, (C) 3 mg mL^{-1}, (D) 4 mg mL^{-1}, (E) 5 mg mL^{-1} and (F) 6 mg mL^{-1}, negative control test and positive control test for 10 min [I] and 120 min [II] incubation time, respectively. Reproduced with permission from Ref. [207]. Copyright 2016, American Chemical Society.

the early stages of the life [197].

The biocompatibility of PANI and its composites was studied both *in vitro* and *in vivo* methods. Nonetheless, a complete investigation of hosting behavior in these materials might be dependent on further experiments to evaluate the biodegradability of the material. Biodegradability is a result of the biologic response of the cells or tissue to the materials used. It should be considered that the conducting polymers, especially those proposed for tissue engineering applications are largely non-biodegradable. Because of such nature, the biodegradability of a PANI-based biomaterial generally can be related to the other component(s) of the system rather than the PANI itself. Blending or copolymerization of PANI with other biodegradable and biocompatible polymers as if PCL and PLA are the most tried solves for this problem [223]. An excellent information about the interaction of cells with hosting materials has been reported by Miyoshi [224]. Also, important discussion about the biodegradability of conductive materials has already been done by Wang et al. [225].

The biocompatibility of the PANI-based biomaterials was evaluated in the contact with different cell lines and alive models. These materials can actually be applied as the biomaterials, especially for cells or tissues

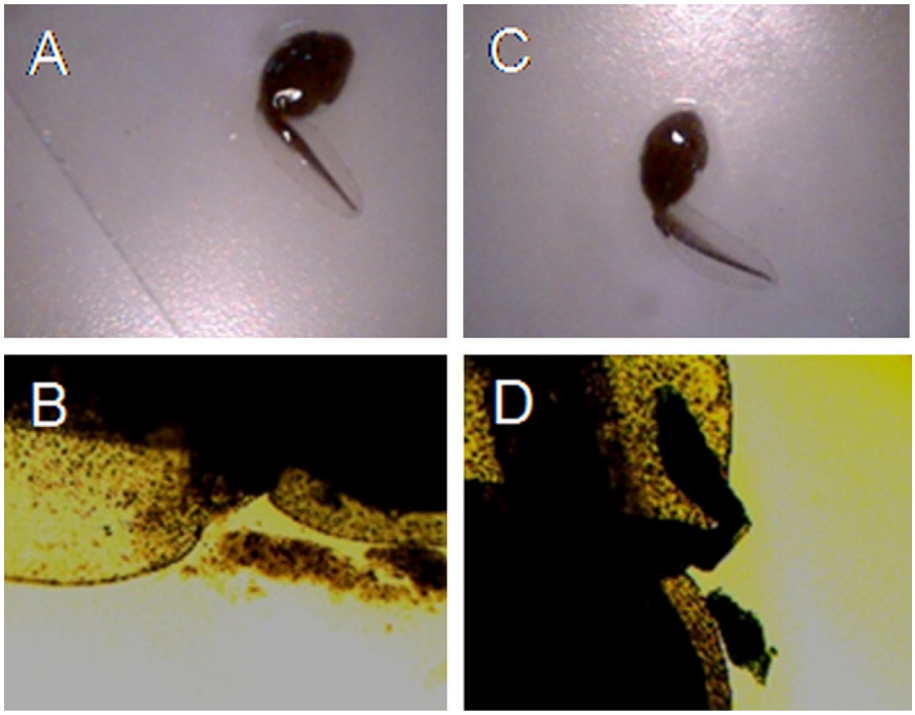

Fig. 4. Optical micrographs of *Rhinella arenarum* larvae grown: (A) and (B) with food fish; (C) and (D) with PANI nanofibers as the only carbon source. Reproduced with permission from Ref. [197]. Copyright 2012, Elsevier.

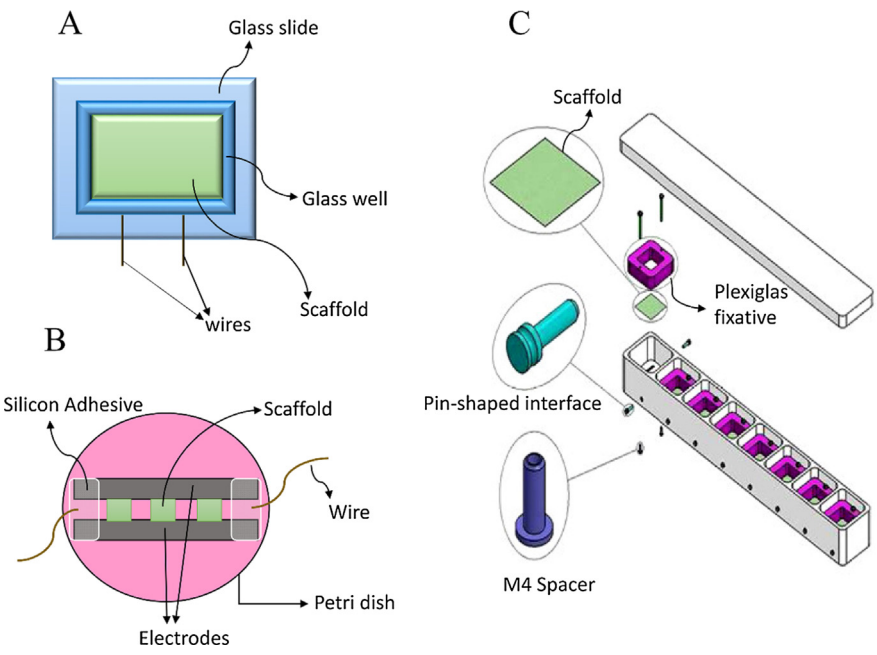

Scheme 4. Different bioreactors, developed by scholars. (A) 1 × 1 cm glass cell; reproduced from Ref. [190]. (B) Custom-made bioreactor fixed into a Petri dish; reproduced from Ref. [231]. (C) Computer designed eight-well bioreactor. Reproduced with permission from Ref. [210]. Copyright 2017, American Chemical Society.

to respond to the electrical current. The exact biocompatibility of the PANI-based materials appears to be dependent on the biologic specifics and should be studied for any cell line, tissue or model separately.

5. Electrical stimulation: a specific application

Biocompatible polymeric composites of IEPs, theoretically, have the potential to be applied as a scaffold in the field of tissue engineering. Such scaffolds provide biocompatible entities for the biological activities, proliferation, differentiation of cells, and hence, may modulate the functions of tissue/organ. Growth factors, antibiotics, and other supplements help the scaffold to perform its function. Nonetheless, when an engineered scaffold benefits an electroconductive component in its composition, it provides an exclusive opportunity. Such scaffold can substitute the growth factors and many other supplements with the electrical current provided to appropriate cell type *per se*. The ES, in fact, is a proprietary application for the scaffolds that benefit from the IEPs in their structure, which are discussed in details in the following section.

5.1. Electrical stimulation: how does it work?

It has been shown that the treatment of cells cultured on the electroconductive platforms by the electricity may affect their biologic behavior(s). In 1997, Schmidt and coworkers released the first scientific report related to the effect of ES on cells [226]. They showed that the PC-12 cells cultured on the PP films and subjected to the electrical stimulus displayed longer neurite as compared to the cells not treated with the electrical stimulation and the untreated control cells cultured on tissue culture PS. A number of similar studies with other nerve cell lines or other electroconductive materials were reported later on [227–229]. For instance, the utility of the ES proved in the cardiac tissue and heart engineering [230–232]. The usefulness of the ES utility in the cardiac tissue engineering has been well discussed by Bidez et al. [233].

The logic behind the ES process is based on the role of bioelectricity in the human body. Since, in the human body, the bioelectricity has fundamental roles in the maintaining normal biologic activities of the cells, including cell signaling in the nerve cells, muscle contraction, and wound healing. As a result, much attention was paid to the treatment of various cells by the electricity using electroconductive biomaterials [61]. Mechanisms of the ES effect on cells have already been discussed by Pires et al. These researchers have remarked that the ES can regulate the intracellular signaling pathways, increase the protein biosynthesis, and favor the ECM protein conformation changes [234].

In a remarkable investigation, Gu et al. showed that peripheral blood stem cells of Sprague-Dawley rats can proliferate and differentiate to Schwann cells under the ES. In this work, a low-frequency electrical stimulation applied for 1 h (20 Hz, 100 μs, 3 V) was shown to improve the cell proliferation and induce the differentiation of peripheral blood stem cells to Schwann cells. To detect and evaluate the mechanism of the ES effect on the cells, the functional expressions of ERK 1/2, p-ERK 1/2, CyclinD1 and CDK4 were studied in four different groups of cells, including (a) ERK-blockage group, (b) low-frequency ES group, (c) low-frequency ES + ERK-blockage group and (d) control group with no intervention. It was reported that the ES process could affect the cells by the ERK signaling pathway. Since the Schwan cells are one of the most preferred sources in the repair of the central and peripheral nerve injuries, this study highlighted the role of the ES in the regenerative medicine [235]. Beyond the cellular level, it was considered that improvement in the cell-cell communication might provide some therapeutic opportunities in the regeneration of engineered tissues, in large part because of the ES [230,232].

The ES provides a specific application for the electrically conductive biomaterials, by which differentiation of cells and tissues can be facilitated. The application of ES has attracted much more attention in the field of the regenerative medicine. However, the application of electricity to cells or injured tissue may confront with some technical challenges such as the requirements for the development of an appropriate bioreactor, optimization of the effective modules for inducing the electrical current, and improvement of the conditions of stimulation. Hence, the ES process may require appropriate requirements such as the implementation of bioreactors.

5.1.1. Challenge for the development of an appropriate bioreactor

Preparation of a proper setup for the ES is a practical challenge. A bioreactor is necessary to treat the cells/tissue. Such bioreactor must have compliance with biologic medium and must effectively transfer the electricity to the cells or tissue. The aseptic condition should be established in every part of the bioreactor to eliminate any effects of the presence of bioreactor.

Any research group should optimize the ES “setup” for any specific

study. Custom-made or commercially available prototypes of electrical devices may carry out the ES process. Scheme4 shows some bioreactors fabricated by scholars in different studies from the simplest to most complex bioreactors.

Hsiao and coworkers overcome the bioreactor challenge by implementing some simple aspects. In their work, the prepared scaffold was placed on a glass slide and two silver wires located under two ends of the scaffold. This assemble was covered using a glass well (1 × 1 cm inner well dimension), while the whole chamber was tightly sealed by the silicon paste [199].

Tandon and coworkers seeded cells onto collagen sponges, transferred them to a petri dish with 6 cm in diameter. Electrical field stimulated using two rod-shaped electrodes (4 cm length, 1/8 in. diameter, placed 1 cm apart), connected by silicon adhesive to each other and by platinum wires to the stimulator (for details see Scheme 4) [231]. In a similar approach, Hirt et al. developed a custom-made electrical pacing unit. Four pairs of carbon electrodes, as a scaffold, were connected to two stainless steel square bars with the certain thickness and certain distances. The unit was applied to the wells of a standard 24-well plate. Using 6 units, parallel to each other, all of the cells in 24-well plate were shown to be stimulated [232].

A 4 × 4 well bioreactor designed and fabricated from PDMS by Serena et al for the application of ES on the hESCs. The bioreactor was fabricated by applying stereolithography via curing the PDMS in a mold. Two sides of each row could accept the electrode with 1.3 mm in diameter and then any row contributes in the stimulation, independently to others [236].

An eight-well bioreactor designed by 3D CAD software (SOLIDWORKS) and manufactured from plexiglas using CNC machinery by Mohammadi-Amirabad et al. In any well of this bioreactor, there is a pair of pin-shaped interfaces, through which stainless steel electrodes (1.4 mm in diameter and 25 mm length) inserted to the well. There is a square-shaped fixative in each well to uniformly connecting fabricated scaffold to the electrodes. Having capitalized on such an arrangement, the researchers showed that the ES was applicable in each well (see Scheme 4) [210].

Taken all, to resolve the bioreactor challenge, each case needs to be optimized *per se* based on the condition and nature of the experiment.

5.2. Electrical stimulation using PANI-based biomaterials

As mentioned earlier, bioelectricity exists within the signaling pathways among the nerve cells, contraction of muscle cells and wound healing in injured tissues. On the other hand, the application of ES can result in mimicking the original activation of bioelectricity. As a result, the cells which play the main roles in bioelectrical activities are the most preferred types in the ES process.

The ES has been applied to the stem cells with different sources, myoblasts, fibroblast and neural cells using well-characterized PANI-based biomaterials as the scaffold. In some studies, the cell behavior under the ES was monitored and compared with the control cells without enduring ES. The PANI-involved scaffolds in these studies exhibited significant ability in terms of hosting and possibly differentiating the cells.

An implicate of the ES process on rat nerve stem cells (C17.2) was reported by Prabhakaran and coworkers. They used electrospun PLLA/PANI blend fibers at a ratio of 85:15 as the scaffold. After 24 h of cell seeding, the ES process carried out for 60 min at a constant electric field of 100 mV/mm. A significant increase in the length of the neuritis observed because of the ES process (24 ± 4ìm with ES compare with 15 ± 3ìm without ES) (see Fig. 5) [195]. Once compared to a former study conducted by the same group in which the same cells were seeded on a PCL/gelatin/PANI nanofibrous scaffold, the obtained results showed remarkable improvements. The electrical conductivity of PCL/gelatin/PANI scaffold was measured to be about 20×10^{-6} S, while the electrical conductivity of PLLA/PANI scaffold was around 3×10^{-6} S. Thus, the PCL/gelatin/PANI scaffold was considered as a suitable setting for transferring of the applied electrical current during the ES process. Furthermore, a longer neurite was observed in the case of PCL/gelatin/PANI, which was equal to 30 ± 1ìm [61]. This comparison obviously highlights the significant role of the ES process in the regeneration purposes. More conductive scaffold causes more effective ES for the cells, and hence, longer neuritis. More extended neurite networks resulted from the ES process in both study reveal the impact of the ES in the nerve tissue regeneration.

Morphological changes detected in the hMSCs. After 7 days of electrical stimulation, the ES resulted in differentiation of the hMSC to the neuron-like cells even in the case of the highly doped substrate [201]. Thrivikraman and coworkers studied the hMSCs viability, proliferation, and differentiation on PANI substrate with different concentration of HCL dopant. It was reported that, when the concentration of dopant increases in substrate structure, the number of cells was decreased and the viability of cells was negatively affected. The cells were stimulated with an intermittent pattern of the electric field (dc) for 7 days (100 mV cm^{-1} for 10 min/day after cell seeding). Although the cell viability did not improve despite the ES because of dopant presence in high concentration; the cells stimulated by the electricity showed obvious differentiation into the neuron-like morphology. This remarkable observation illustrates the undoubtful role of ES in the cell differentiation. This group developed their work toward studying the ES effect on other stem cell lines using PANI-based biomaterials as substrate. To this end, they developed a PANI-based biomaterial by coating a PANI substrate with Coll1 alone or in associated with sHya which forms an aECM. The engineered aECM was shown to mimic the native microenvironment of bone tissue. Moderate conductivity in the range of 10^{-4}–10^{-3} S cm^{-1} was reported for the developed biomaterial. Similar to the previous work [201], the hMSCs were cultured on prepared biomaterials and their differentiation to the bone tissue was investigated by studying the gene expression of bone markers. The ES process performed using the PEF (7 ms rectangular pulses, 3.6 mV cm^{-1}, 10 Hz). In the presence of PEF, the gene expression of Coll1A1, OPN and RUNX2 were reported to be similar to that of the untreated cells. Further, the expressions of ALP and OCN significantly were found to be improved in the case of the PEF treated cells on aECM substrates. The cell morphology and growth were markedly improved by the PEF treating. Star-shaped cells with an increased occupied area were observed in the presence of PEF (Fig. 5). The mechanism of ES effect was found on the cell morphology that might be accomplished by two manners, including (a) PEF prepared cues that assemble and disassembly of actin performed upon them and (b) PEF affect the local electric field of ECM, resulting in the redistribution of cell receptors, an therefore cell behavior. It should be noted that the ES process has not affected the cell proliferation, while the PANI/Coll/sHya scaffold enhanced the cell proliferation capacity up to 28 days even in the absence of ES [205].

The PANI-based biomaterials were engineered in the form of “electrodes” and then applied for the ES on different tissues. For example, Min and coworkers investigated the ES process using sulfonated-PANI based biomaterials as electrodes. They investigated the effect of ES process on different cell lines related to the bone tissue, including BMSCs, pre-osteoblast cells (MC3T3-E1) and the HOSCs [237,238].

Zhang et al. reported a synergic effect of the ES and NGF on the differentiation of rat PC12 cells. In this study, the PC12 cells cultured on the electrospun PANI associated with PSK blends with a different composition. The NGF loaded into the prepared polymeric systems and 24 h after seeding, then the cells were stimulated with 100 mV cm^{-1} for 5 h per day (total 5 days). Neurite outgrowth was analyzed under consideration of NGF release from the scaffolds and the application of ES. Having compared the PS/PANI and NGF-loaded-PS/PANI, an increase was found in median neurite length from 7.5 to 19.7 μm. The percentage of the neuritis was recorded in the range from 1.5 ± 1.2% to 29.7 ± 2.1% under the ES condition. The ES also improved the NGF

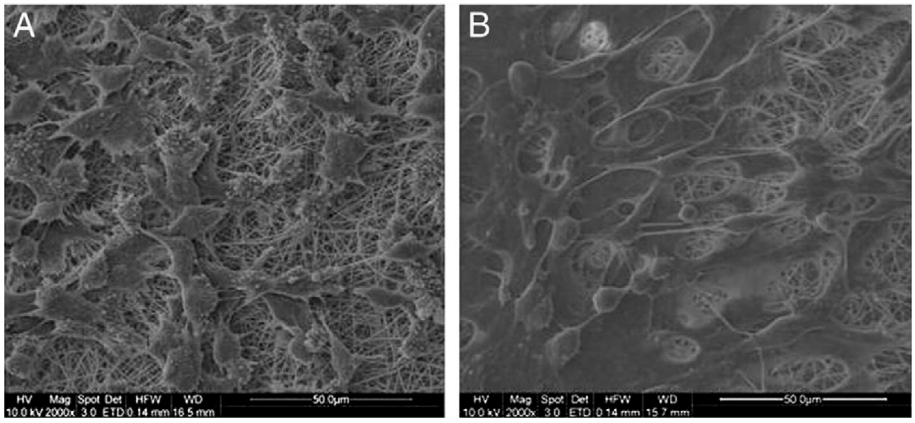

Fig. 5. The scanning electron microscopy images of nerve stem cells on PLLA/PANI nanofibers. (A) Non-stimulated. (B) Electrically stimulated for 60 min period. Reproduced with permission from Ref. [195]. Copyright 2011, Elsevier.

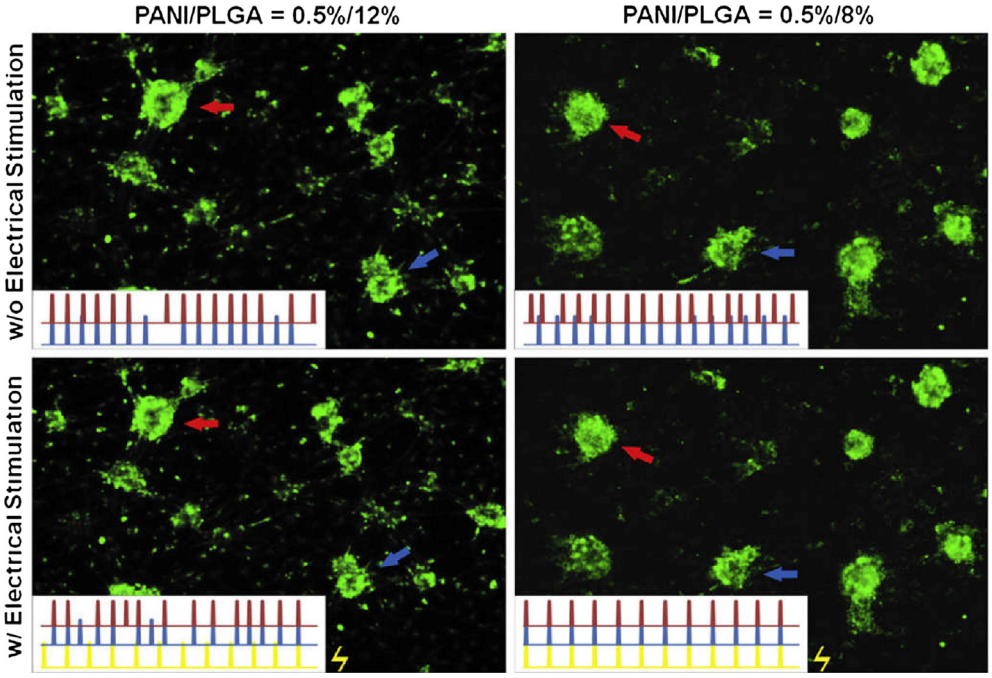

Fig. 6. The beating frequencies (BFs) of isolated cell clusters. The BFs in the images indicated by the red and blue arrows for the cells grown on the low- and high-conductivity meshes (PNAI/PLGA ¼ 0.5%/12% and 0.5%/8%, respectively) before and after the electrical stimulation. The electrical potential frequency was denoted by the yellow line (the one with the yellow lightning symbol). For details, the readers are referred to the web version of the article. Reproduced with permission from Ref. [199]. Copyright 2013, Elsevier. (For interpretation of the references to color in this figure legend, the reader is referred to the web version of this article.)

release from the NGF-loaded-PS/PANI fibers. Based on this observation, the prepared biomaterials were suggested to be applied in electro-responsive drug delivery systems [239].

In another work, Wang et al. coated an ITO glass with PANI. Then, to evaluate the biocompatibility of the engineered materials, they analyzed adsorbed protein by PC-12 cells using SDS-PAGE method both in the presence and absence of the ES. About 24 h post-seeding, the cells were treated by rectangular electric pulses with an amplitude of 100 μA and pulse width of 0.8. The pulses were repeated each second for 1, 2, and 4 h. Using MTT assay, a significant difference was reported for the ES treatment, in which values related to 4 h stimulation did not differ from that of 2 h. Similar to other reports, the ES caused an increase in the neurite outgrowth. In this work, protein adsorption in DMEM media was investigated based on the fact that protein adsorption might occur when the biomaterial surface is exposed to the biologic medium. This phenomenon appears to affect the adhesion of the cell and following responses such as inflammatory. After 4 h of stimulation, the amount of the adsorbed protein was monitored using AFM microscopy. The SDS-PAGE analyses in this study showed a new band (band 2, about 37 kDa) after the cell culture, which was secreted by the PC-12 cells. Furthermore, an increase in the secreted protein related to band 1 (around 90 kDa) was observed after 4 h of stimulation. These results demonstrate that the mechanism of the ES process on the nerve cells might involve in the increased adsorption of ECM proteins such as fibronectin [240].

Since the native function of cardiac tissue fundamentally depends on the bioelectricity, this tissue is a preferred candidate for the investigation of the ES process. In a study, Hsiao and coworkers isolated the neonatal cardiomyocytes from the hearts of 1–2 day old rats [199]. The cells were then cultured on the electrospun PANI/PLGA nanofibers and treated with the ES process. Characteristic electrical pulses of the native myocardium (1.25 Hz, 5 V cm^{-1}) were applied to the cells. Beating rates of the cultured cells were synchronized with the ES pulses and analyzed with high-speed photography. The cell clusters were cultured on two different meshes with different percentage of involved PANI; and thus, different conductivity. The cells cultured on both low- and high-conductive meshes were found to beat asynchronously before the ES. After the ES process, as shown in Fig. 6, the beating frequency was relatively improved in the cells cultured on the low-conductive mesh and even was the same as that of the oscillation of the electrical potential [199]. These findings show the significant role of the ES treatment in coordinating the connection between the cardiac cells.

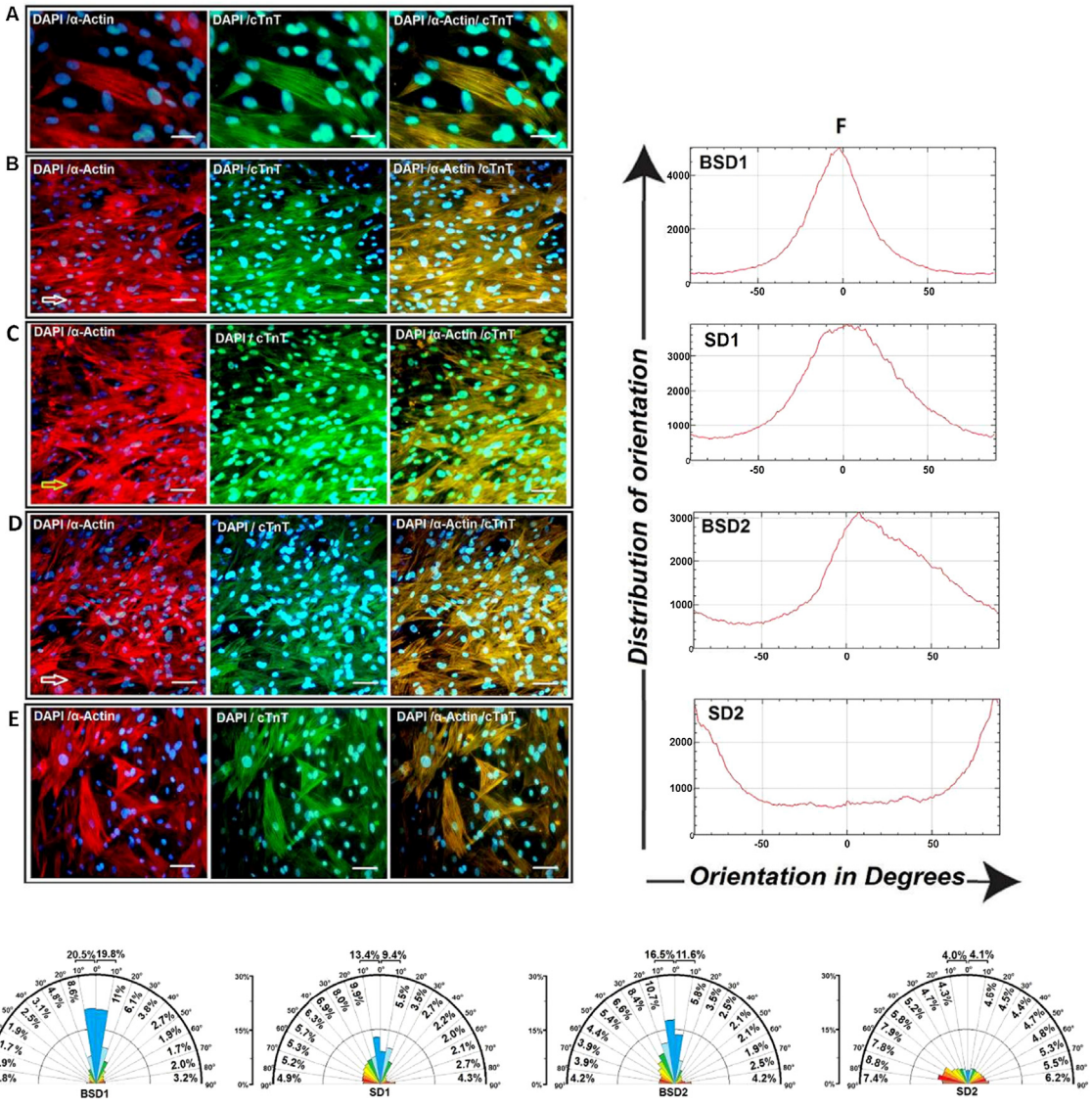

Fig. 7. The immunofluorescence stained images of cardiac-specific structural entities such as α-actin and cTnT in (A) cardiomyocyte-like cell (zoom in view). The cells cultured on aligned and PANI/PES nanofibrous scaffolds (B) with and (C) without electrical stimulation. The cells cultured on random PANI/PES nanofibrous scaffolds (D) with and (E) without electrical stimulation. (F) The distribution of orientations against orientation of cells in the experimental groups. (G) The quantitative analysis of cellular alignment in the angle of 0–90° in both directions. The white arrows showed the electrical pulse orientation and a cyan arrow showing the orientation of fibers in the scaffold. Scale bars = 20 μm (A) and 100 μm (B–E). Reproduced with permission from Ref. [210]. Copyright 2017, American Chemical Society.

Li et al. investigated the effect of ES on the HUVECs under conditions of the stimulating with 200, 300 and 400 mV cm^{-1}. The cytoskeleton organization of the cells cultured on PCL and PCL/PANI nanofibers was studied by rhodamine-phalloidine staining. Under the ES condition, especially using 400 mV cm^{-1}, the HUVECs have shown enhanced adhesion and viability. In addition, in the presence of the ES process, morphological analysis using SEM technique was performed for the cells cultured on the PCL/PANI mesh compared to those of cultured on the PCL alone. The comparison approved that the function of PANI was found to facilitate the cell proliferation and improve the morphology [209].

The cardiovascular cell morphology has been shown to be remarkably influenced by the direction of the fibrous substrate in numerous studies. For example, Ku et al. clarified the effects of electrospun PANI/PCL nanofibers, while the alignment of the nanofibers and the concentration of PANI did not show significant influence on the cell growth and proliferation. Nevertheless, the direction of the fibrous substrate affects the morphology of the cells. Further, bipolar and multipolar structures were observed for the cells cultured on random and aligned fibrous substrates, respectively [241].

The effect of the direction of ES, by which the electric current induces to cells, was highlighted by Mohammadi Amirabad et al. They used aligned and random PANI/PES nanofibers. In this study, CVD-iPSCs were isolated from the fibroblasts of the patients, who were undergone cardiothoracic surgeries. The obtained cells cultured on the fabricated aligned and random scaffolds using a modified minimum medium as well as differentiation medium for 5 days. The investigation was performed under the ES condition by square-wave impulses (1 Hz for 2 ms and 50 mV cm^{-1}) 1 h per day for 15 days as well as the lack of the ES process. About 21 days after cell seeding, immunofluorescence staining of the cardiac-specific structural markers, including α-actin and cTnT, was performed to evaluate the results of the obtained differentiation (Fig. 7). The highest differentiation to cTnT + cells resulted when the ES process applied using the aligned PANI/PES [210].

Since the bioelectricity has an intrinsic role in the wound healing, the cells contributing to the wound healing are remarkable candidates

for the ES process. Following this logic, Petrov et al. studied the effect of the ES on L929 fibroblast cells cultured on HEC/PANI cryogels. MTT assay approved satisfying viability for the cells cultured on the fabricated electroconductive cryogel substrate. The cells were cultured on 1% and 2% PANI substrates and treated with 2.5 V cm^{-1} electrical fields for 24 h. The L929 cells under ES condition were shown to have a tendency for positioning near the cathode. This behavior was speculated to occur because of the charged polarons (cation radicals) contained in the structure of PANI [208].

The ES process is a tool for managing of the cellular behaviors. The application of this tool in a body might be conditional to a much more accurate and effective control of the cellular functions. Such control becomes possible by the design of multi-stimuli responsive materials scaffolds. Then, the introduction of biomaterials with another kind of stimuli besides the ES should be considered as the next goal in this field [225]. Additionally, such managed biomaterials might practically be useful only after the complete *in-vivo* evaluations and clinical trials for electroconductive biomaterials. Up to now, there are no FDA-approved PANI-based scaffolds and none of the synthesized PANI-based biomaterials has been introduced to the clinical trials yet. Thus, future PANI-based biomaterials have to pass required standards for the use in the human or other alive models. The useful and precise discussion is available by Hardy et al. in terms of the f the biomimetic conducting polymers used as tissue scaffolds [242].

6. Final remarks and conclusions

The PANI-based biomaterials have approved their application in bioscience as well as other implementations. Although *in-vitro* biocompatibility of the PANI-based materials depends on the cell type, further investigations seem to be necessary to fully address all aspects of these advanced materials. Engineering, application, and marketing of the materials with optimum conductivity-biocompatibility balance appear to be the main challenge in this area. We envision that the PANI-based electroconductive implants will be commercially available in the near future. Such advanced systems can become a game changer in the regenerative medicine, in part because of their electrical biomimetic characteristics, even though their industrial scale-up and marketing still remain as big challenges.

References

[1] Search Analysis for “Biomaterials” in SCOPUS. < https://www.scopus.com/term/analyzer.uri?sid=698B3F4E8CBFB9E6FD9C90104B6D158D.wsnAw8kcdt7IPYLO0V48gA%3a90&origin=resultslist&src=s&s=TITLE-ABS-KEY%28Biomaterials%29&sort=plf-f&sdt=b&sot=b&sl=27&count=54321&analyzeResults=Analyze+results&txGid=698B3F4E8CBFB9E6FD9C90104B6D158D.wsnAw8kcdt7IPYLO0V48gA%3a13#spreadsheet > . (accessed August 7 2018).
[2] Biomaterials Market by Type of Materials (Metallic, Ceramic, Polymers, Natural) & Application (Cardiovascular, Orthopedic, Dental, Plastic Surgery, Wound Healing, Neurology, Tissue Engineering, Ophthalmology) - Global Forecast to 2021 2016. < http://www.marketsandmarkets.com/Market-Reports/biomaterials-393.html > . (accessed December 2016 2016).
[3] B.D. Ratner, The Nature of Matter and Materials, Biomaterials Science, third ed., Academic Press, 2013, pp. 6–9 (Chapter I.1.2).
[4] D.F. Williams, B. European Society for, Definitions in Biomaterials : Proceedings of a Consensus Conference of the European Society for Biomaterials, Chester, England, March 3–5, 1986, Elsevier, Amsterdam; New York.
[5] Introduction, Biomaterials, Springer, New York, 2007, pp. 1–16.
[6] S. Camarero-Espinosa, J. Cooper-White, Tailoring biomaterial scaffolds for osteochondral repair, Int. J. Pharm. 523 (2) (2017) 476–489.
[7] S.I. Ivanova, S. Chakarov, A. Momchilova, R. Pankov, Live-cell biosensor for assessment of adhesion qualities of biomaterials, Mater. Sci. Eng. C 78 (2017) 230–238.
[8] A.M. Pereira, R. Machado, A. da Costa, A. Ribeiro, T. Collins, A.C. Gomes, I.B. Leonor, D.L. Kaplan, R.L. Reis, M. Casal, Silk-based biomaterials functionalized with fibronectin type II promotes cell adhesion, Acta Biomater. 47 (2017) 50–59.
[9] L.G. Bracaglia, M. Messina, C. Vantucci, H.B. Baker, A. Pandit, J.P. Fisher, Controlled delivery of tissue inductive factors in a cardiovascular hybrid biomaterial scaffold, ACS Biomater. Sci. Eng. (2016).
[10] I.C. Gonçalves, A. Magalhães, A.M.S. Costa, J.R. Oliveira, P.C. Henriques, P. Gomes, C.A. Reis, M.C.L. Martins, Bacteria-targeted biomaterials: glycan-coated microspheres to bind Helicobacter pylori, Acta Biomater. 33 (2016) 40–50.
[11] E.R. Cervantes, M.G. Torres, S.V. Muñoz, E.R. Rosas, C. Vázquez, R.R. Talavera, Growth of hydroxyapatite on the cellular membrane of the bacterium Bacillus thuringiensis for the preparation of hybrid biomaterials, Mater. Sci. Eng. C 58 (2016) 614–621.
[12] M. Parlato, J. Molenda, W.L. Murphy, Specific recruitment of circulating angiogenic cells using biomaterials as filters, Acta Biomater. 56 (2017) 65–79.
[13] K. Chawla, Biomaterials for tissue engineering and regenerative medicine: treatment of musculoskeletal injury and disease, Mater. Sci. Eng. A 557 (2012) 45–53.
[14] Y.E. Arslan, T. Sezgin Arslan, B. Derkus, E. Emregul, K.C. Emregul, Fabrication of human hair keratin/jellyfish collagen/eggshell-derived hydroxyapatite osteoinductive biocomposite scaffolds for bone tissue engineering: from waste to regenerative medicine products, Colloids Surf. B. Biointerfaces 154 (2017) 160–170.
[15] M.E. Furth, A. Atala, M.E. Van Dyke, Smart biomaterials design for tissue engineering and regenerative medicine, Biomaterials 28 (34) (2007) 5068–5073.
[16] B. Akar, B. Jiang, S.I. Somo, A.A. Appel, J.C. Larson, K.M. Tichauer, E.M. Brey, Biomaterials with persistent growth factor gradients in vivo accelerate vascularized tissue formation, Biomaterials 72 (2015) 61–73.
[17] J. Grzesiak, K. Marycz, D. Szarek, P. Bednarz, J. Laska, Polyurethane/polylactide-based biomaterials combined with rat olfactory bulb-derived glial cells and adipose-derived mesenchymal stromal cells for neural regenerative medicine applications, Mater. Sci. Eng. C 52 (2015) 163–170.
[18] Z. Cui, B. Yang, R.-K. Li, Application of biomaterials in cardiac repair and regeneration, Engineering 2 (1) (2016) 141–148.
[19] G.T. Tihan, I. Rău, R.G. Zgârian, M.V. Ghica, Collagen-based biomaterials for ibuprofen delivery, C.R. Chim. 19 (3) (2016) 390–394.
[20] A.D. Friedman, D. Kim, R. Liu, Highly stable aptamers selected from a 2′-fully modified fGmH RNA library for targeting biomaterials, Biomaterials 36 (2015) 110–123.
[21] M.A. Tölli, M.P.A. Ferreira, S.M. Kinnunen, J. Rysä, E.M. Mäkilä, Z. Szabó, R.E. Serpi, P.J. Ohukainen, M.J. Välimäki, A.M.R. Correia, J.J. Salonen, J.T. Hirvonen, H.J. Ruskoaho, H.A. Santos, In vivo biocompatibility of porous silicon biomaterials for drug delivery to the heart, Biomaterials 35 (29) (2014) 8394–8405.
[22] D.S. Jones, G.P. Andrews, D.L. Caldwell, C. Lorimer, S.P. Gorman, C.P. McCoy, Novel semi-interpenetrating hydrogel networks with enhanced mechanical properties and thermoresponsive engineered drug delivery, designed as bioactive endotracheal tube biomaterials, Eur. J. Pharm. Biopharm. 82 (3) (2012) 563–571.
[23] C. Garcia-Mazas, N. Csaba, M. Garcia-Fuentes, Biomaterials to suppress cancer stem cells and disrupt their tumoral niche, Int. J. Pharm. 523 (2) (2017) 490–505.
[24] J. Rnjak-Kovacina, L.S. Wray, K.A. Burke, T. Torregrosa, J.M. Golinski, W. Huang, D.L. Kaplan, Lyophilized silk sponges: a versatile biomaterial platform for soft tissue engineering, ACS Biomater. Sci. Eng. 1 (4) (2015) 260–270.
[25] L. Davenport Huyer, B. Zhang, A. Korolj, M. Montgomery, S. Drecun, G. Conant, Y. Zhao, L. Reis, M. Radisic, Highly elastic and moldable polyester biomaterial for cardiac tissue engineering applications, ACS Biomater. Sci. Eng. 2 (5) (2016) 780–788.
[26] Y. Gao, E.P. Childers, M.L. Becker, l-Leucine-based poly(ester urea)s for vascular tissue engineering, ACS Biomater. Sci. Eng. 1 (9) (2015) 795–804.
[27] R.D. Abbott, E.P. Kimmerling, D.M. Cairns, D.L. Kaplan, Silk as a biomaterial to support long-term three-dimensional tissue cultures, ACS Appl. Mater. Interfaces 8 (34) (2016) 21861–21868.
[28] T.J. Keane, S.F. Badylak, Biomaterials for tissue engineering applications, Semin. Pediatr. Surg. 23 (3) (2014) 112–118.
[29] N. Jornet-Martínez, P. Campíns-Falcó, E.A.H. Hall, Zein as biodegradable material for effective delivery of alkaline phosphatase and substrates in biokits and biosensors, Biosens. Bioelectron. 86 (2016) 14–19.
[30] Y. Wang, X. Huang, H. Li, L. Guo, Sensitive impedimetric DNA biosensor based on (Nb, V) codoped TiO2 for breast cancer susceptible gene detection, Mater. Sci. Eng. C 77 (2017) 867–873.
[31] N. Hui, X. Sun, S. Niu, X. Luo, PEGylated polyaniline nanofibers: antifouling and conducting biomaterial for electrochemical DNA sensing, ACS Appl. Mater. Interfaces 9 (3) (2017) 2914–2923.
[32] B.D. Lawrence, M. Cronin-Golomb, I. Georgakoudi, D.L. Kaplan, F.G. Omenetto, Bioactive silk protein biomaterial systems for optical devices, Biomacromolecules 9 (4) (2008) 1214–1220.
[33] L.V. Sigolaeva, S.Y. Gladyr, A.P.H. Gelissen, O. Mergel, D.V. Pergushov, I.N. Kurochkin, F.A. Plamper, W. Richtering, Dual-stimuli-sensitive microgels as a tool for stimulated spongelike adsorption of biomaterials for biosensor applications, Biomacromolecules 15 (10) (2014) 3735–3745.
[34] K.V. Nguyen, Y. Holade, S.D. Minteer, DNA redox hydrogels: improving mediated enzymatic bioelectrocatalysis, ACS Catal. 6 (4) (2016) 2603–2607.
[35] L. Hench, Biomaterials, Science 208 (4446) (1980) 826–831.
[36] L. Hench, J. Wilson, Surface-active biomaterials, Science 226 (4675) (1984) 630–636.
[37] H.L. Jang, K. Lee, C.S. Kang, H.K. Lee, H.-Y. Ahn, H.-Y. Jeong, S. Park, S.C. Kim, K. Jin, J. Park, T.-Y. Yang, J.H. Kim, S.A. Shin, H.N. Han, K.H. Oh, H.-Y. Lee, J. Lim, K.S. Hong, M.L. Snead, J. Xu, K.T. Nam, Biofunctionalized ceramic with self-assembled networks of nanochannels, ACS Nano 9 (4) (2015) 4447–4457.
[38] M. Nakamura, R. Hiratai, T. Hentunen, J. Salonen, K. Yamashita, Hydroxyapatite with high carbonate substitutions promotes osteoclast resorption through osteocyte-like cells, ACS Biomater. Sci. Eng. 2 (2) (2016) 259–267.
[39] Y.-G. Zhang, Y.-J. Zhu, F. Chen, Novel interconnected nanochannel hydroxyapatite ceramics: synthesis, microstructure, and permeability, Ceram. Int. 43 (7) (2017)

5403–5411.
[40] B. Rahmati, E. Zalnezhad, A.A.D. Sarhan, Z. Kamiab, B. Nasiri Tabrizi, W.A.B.W. Abas, Enhancing the adhesion strength of tantalum oxide ceramic thin film coating on biomedical Ti–6Al–4V alloy by thermal surface treatment, Ceram. Int. 41 (10 Part A) (2015) 13055–13063.
[41] C. Ritzberger, M. Schweiger, W. Höland, Principles of crystal phase formation in Ivoclar Vivadent glass-ceramics for dental restorations, J. Non-Cryst. Solids 432 (Part A) (2016) 137–142.
[42] L. Fiocco, L. Ferroni, C. Gardin, B. Zavan, M. Secco, S. Matthews, E. Bernardo, Wollastonite-diopside glass-ceramic foams from supercritical carbon dioxide-assisted extrusion of a silicone resin and inorganic fillers, J. Non-Cryst. Solids 443 (2016) 33–38.
[43] N. Jmal, J. Bouaziz, Synthesis, characterization and bioactivity of a calcium-phosphate glass-ceramics obtained by the sol-gel processing method, Mater. Sci. Eng. C 71 (2017) 279–288.
[44] A. Beilvert, F. Chaubet, L. Chaunier, S. Guilois, G. Pavon-Djavid, D. Letourneur, A. Meddahi-Pellé, D. Lourdin, Shape-memory starch for resorbable biomedical devices, Carbohydr. Polym. 99 (2014) 242–248.
[45] G. Novajra, J. Lousteau, D. Milanese, C. Vitale-Brovarone, Resorbable hollow phosphate glass fibers as controlled release systems for biomedical applications, Mater. Lett. 99 (2013) 125–127.
[46] S. Langstaff, M. Sayer, T.J.N. Smith, S.M. Pugh, Resorbable bioceramics based on stabilized calcium phosphates. Part II: evaluation of biological response, Biomaterials 22 (2) (2001) 135–150.
[47] S. Langstaff, M. Sayer, T.J.N. Smith, S.M. Pugh, S.A.M. Hesp, W.T. Thompson, Resorbable bioceramics based on stabilized calcium phosphates. Part I: rational design, sample preparation and material characterization, Biomaterials 20 (18) (1999) 1727–1741.
[48] F. Taraballi, S. Minardi, B. Corradetti, I.K. Yazdi, M.A. Balliano, J.L. Van Eps, M. Allegri, E. Tasciotti, Potential avoidance of adverse analgesic effects using a biologically “smart” hydrogel capable of controlled bupivacaine release, J. Pharm. Sci. 103 (11) (2014) 3724–3732.
[49] E. Ceci-Ginistrelli, C. Pontremoli, D. Pugliese, N. Barbero, N.G. Boetti, C. Barolo, S. Visentin, D. Milanese, Drug release kinetics from biodegradable UV-transparent hollow calcium-phosphate glass fibers, Mater. Lett. 191 (2017) 116–118.
[50] E.M. Pritchard, T. Valentin, D. Boison, D.L. Kaplan, Incorporation of proteinase inhibitors into silk-based delivery devices for enhanced control of degradation and drug release, Biomaterials 32 (3) (2011) 909–918.
[51] Y. Hu, S. Zou, W. Chen, Z. Tong, C. Wang, Mineralization and drug release of hydroxyapatite/poly(l-lactic acid) nanocomposite scaffolds prepared by Pickering emulsion templating, Colloids Surf. B. Biointerfaces 122 (2014) 559–565.
[52] M.C. Costache, A.D. Vaughan, H. Qu, P. Ducheyne, D.I. Devore, Tyrosine-derived polycarbonate-silica xerogel nanocomposites for controlled drug delivery, Acta Biomater. 9 (5) (2013) 6544–6552.
[53] A.M. Zalfen, D. Nizet, C. Jérôme, R. Jérôme, F. Frankenne, J.M. Foidart, V. Maquet, F. Lecomte, P. Hubert, B. Evrard, Controlled release of drugs from multi-component biomaterials, Acta Biomater. 4 (6) (2008) 1788–1796.
[54] P.A. Tarantili, H. Koumoulos, Sustained release of guaifenesin and ipriflavone from biodegradable coatings, Eur. Polym. J. 44 (2) (2008) 444–452.
[55] L.D. Solorio, E.L. Vieregge, C.D. Dhami, P.N. Dang, E. Alsberg, Engineered cartilage via self-assembled hMSC sheets with incorporated biodegradable gelatin microspheres releasing transforming growth factor-β1, J. Control. Release 158 (2) (2012) 224–232.
[56] L.L. Hench, J.M. Polak, Third-Generation Biomedical Materials, Science 295 (5557) (2002) 1014–1017.
[57] A History of Biomaterials A2 - Ratner, Buddy D, in: A.S. Hoffman, F.J. Schoen, J.E. Lemons (Eds.), Biomaterials Science (Third Edition), Academic Press2013, pp. xli–liii.
[58] V. Migonney, History of Biomaterials, Biomaterials, John Wiley & Sons, Inc., 2014, pp. 1–10.
[59] Q. Wang, S. Jamal, M.S. Detamore, C. Berkland, PLGA-chitosan/PLGA-alginate nanoparticle blends as biodegradable colloidal gels for seeding human umbilical cord mesenchymal stem cells, J. Biomed. Mater. Res. A 96 (3) (2011) 520–527.
[60] E.M. Geniès, A. Boyle, M. Lapkowski, C. Tsintavis, Polyaniline: a historical survey, Synth. Met. 36 (2) (1990) 139–182.
[61] L. Ghasemi-Mobarakeh, M.P. Prabhakaran, M. Morshed, M.H. Nasr-Esfahani, S. Ramakrishna, Electrical stimulation of nerve cells using conductive nanofibrous scaffolds for nerve tissue engineering, Tissue Eng. Part A 15 (11) (2009) 3605–3619.
[62] S. Bhadra, N.K. Singha, S. Chattopadhyay, D. Khastgir, Effect of different reaction parameters on the conductivity and dielectric properties of polyaniline synthesized electrochemically and modeling of conductivity against reaction parameters through regression analysis, J. Polym. Sci. Part B: Polym. Phys. 45 (15) (2007) 2046–2059.
[63] M. Jaymand, Recent progress in chemical modification of polyaniline, Prog. Polym. Sci. 38 (9) (2013) 1287–1306.
[64] A.J. Hackett, J. Malmström, J. Travas-Sejdic, Functionalization of conducting polymers for biointerface applications, Prog. Polym. Sci. 70 (2017) 18–33.
[65] J. Zhu, X. Liu, X. Wang, X. Huo, R. Yan, Preparation of polyaniline–TiO_2 nanotube composite for the development of electrochemical biosensors, Sens. Actuators B. Chem. 221 (2015) 450–457.
[66] L. Tang, X. Xie, Y. Zhou, G. Zeng, J. Tang, Y. Wu, B. Long, B. Peng, J. Zhu, A reusable electrochemical biosensor for highly sensitive detection of mercury ions with an anionic intercalator supported on ordered mesoporous carbon/self-doped polyaniline nanofibers platform, Biochem. Eng. J. 117 (Part A) (2017) 7–14.
[67] A. Jasim, M.W. Ullah, Z. Shi, X. Lin, G. Yang, Fabrication of bacterial cellulose/polyaniline/single-walled carbon nanotubes membrane for potential application as biosensor, Carbohydr. Polym. 163 (2017) 62–69.
[68] S. Ameen, M.S. Akhtar, H.S. Shin, Nanocages-augmented aligned polyaniline nanowires as unique platform for electrochemical non-enzymatic glucose biosensor, Appl. Catal. A 517 (2016) 21–29.
[69] S. Bao, M. Du, M. Zhang, H. Zhu, P. Wang, T. Yang, M. Zou, Facile fabrication of polyaniline nanotubes/gold hybrid nanostructures as substrate materials for biosensors, Chem. Eng. J. 258 (2014) 281–289.
[70] L. Al-Mashat, K. Shin, K. Kalantar-zadeh, J.D. Plessis, S.H. Han, R.W. Kojima, R.B. Kaner, D. Li, X. Gou, S.J. Ippolito, W. Wlodarski, Graphene/polyaniline nanocomposite for hydrogen sensing, J. Phys. Chem. C 114 (39) (2010) 16168–16173.
[71] A.D. Chowdhury, A. De, C.R. Chaudhuri, K. Bandyopadhyay, P. Sen, Label free polyaniline based impedimetric biosensor for detection of E. coli O157:H7 Bacteria, Sens. Actuators B. Chem. 171 (2012) 916–923.
[72] P. Teengam, W. Siangproh, A. Tuantranont, C.S. Henry, T. Vilaivan, O. Chailapakul, Electrochemical paper-based peptide nucleic acid biosensor for detecting human papillomavirus, Anal. Chim. Acta 952 (2017) 32–40.
[73] A.P. Mahajan, S.B. Kondawar, R.P. Mahore, B.H. Meshram, P.D. Virutkar, Polyaniline/MnO2 nanocomposites based stainless steel electrode modified enzymatic urease biosensor, Procedia Mater. Sci. 10 (2015) 699–705.
[74] M. Zhybak, V. Beni, M.Y. Vagin, E. Dempsey, A.P.F. Turner, Y. Korpan, Creatinine and urea biosensors based on a novel ammonium ion-selective copper-polyaniline nano-composite, Biosens. Bioelectron. 77 (2016) 505–511.
[75] K.Z. Htut, M. Kim, E. Lee, G. Lee, S.H. Baeck, S.E. Shim, Biodegradable polymer-modified graphene/polyaniline electrodes for supercapacitors, Synth. Met. 227 (2017) 61–70.
[76] A.G. MacDiarmid, A.J. Epstein, Polyanilines: a novel class of conducting polymers, Faraday Discuss. Chem. Soc. 88 (1989) 317–332.
[77] D.D. Zhou, X.T. Cui, A. Hines, R.J. Greenberg, Conducting polymers in neural stimulation applications, in: D. Zhou, E. Greenbaum (Eds.), Implantable Neural Prostheses 2: Techniques and Engineering Approaches, Springer, New York, New York, NY, 2010, pp. 217–252.
[78] Z. Shi, X. Gao, M.W. Ullah, S. Li, Q. Wang, G. Yang, Electroconductive natural polymer-based hydrogels, Biomaterials 111 (2016) 40–54.
[79] H. Peng, X. Liu, G. Wang, M. Li, K.M. Bratlie, E. Cochran, Q. Wang, Polymeric multifunctional nanomaterials for theranostics, J. Mater. Chem. B 3 (34) (2015) 6856–6870.
[80] J. Gong, Y. Li, Z. Hu, Z. Zhou, Y. Deng, Ultrasensitive NH3 gas sensor from polyaniline nanograin enchased TiO2 fibers, J. Phys. Chem. C 114 (21) (2010) 9970–9974.
[81] L. Xue, W. Wang, Y. Guo, G. Liu, P. Wan, Flexible polyaniline/carbon nanotube nanocomposite film-based electronic gas sensors, Sens. Actuators B. Chem. 244 (2017) 47–53.
[82] H.T. Hien, H.T. Giang, N.V. Hieu, T. Trung, C.V. Tuan, Elaboration of Pd-nanoparticle decorated polyaniline films for room temperature NH3 gas sensors, Sens. Actuators B. Chem. 249 (2017) 348–356.
[83] P. Cavallo, E. Frontera, D.F. Acevedo, R. Olejnik, P. Slobodian, P. Saha, C.A. Barbero, Functionalized polyanilines made by nucleophilic addition reaction, applied in gas sensors field, Synth. Met. 215 (2016) 127–133.
[84] K. Ghanbari, Z. Babaei, Fabrication and characterization of non-enzymatic glucose sensor based on ternary NiO/CuO/polyaniline nanocomposite, Anal. Biochem. 498 (2016) 37–46.
[85] S.K. Shukla, M.M. Demir, P.P. Govender, A. Tiwari, S.K. Shukla, Optical fiber based non-enzymatic glucose sensing over Cu2 + -doped polyaniline hybrid matrix, Sens. Actuators B. Chem. 242 (2017) 522–528.
[86] W. Zheng, L. Hu, L.Y.S. Lee, K.-Y. Wong, Copper nanoparticles/polyaniline/graphene composite as a highly sensitive electrochemical glucose sensor, J. Electroanal. Chem. 781 (2016) 155–160.
[87] M. Choudhary, S.K. Shukla, A. Taher, S. Siwal, K. Mallick, Organic-inorganic hybrid supramolecular assembly: an efficient platform for nonenzymatic glucose sensor, ACS Sustain. Chem. Eng. 2 (12) (2014) 2852–2858.
[88] N. Prabhakar, K. Arora, H. Singh, B.D. Malhotra, Polyaniline based nucleic acid sensor, J. Phys. Chem. C 112 (15) (2008) 4808–4816.
[89] T. Yang, L. Meng, J. Zhao, X. Wang, K. Jiao, Graphene-based polyaniline arrays for deoxyribonucleic acid electrochemical sensor: effect of nanostructure on sensitivity, ACS Appl. Mater. Interfaces 6 (21) (2014) 19050–19056.
[90] X. Wang, H. Wang, T. Ge, T. Yang, S. Luo, K. Jiao, Chemically modified graphene and sulfonic acid-doped polyaniline nanofiber composites: preparation routes, characterization, and comparison of direct DNA detection, J. Phys. Chem. C 119 (17) (2015) 9076–9084.
[91] P.P. Sengupta, J.N. Gloria, D.N. Amato, D.V. Amato, D.L. Patton, B. Murali, A.S. Flynt, Utilizing intrinsic properties of polyaniline to detect nucleic acid hybridization through UV-enhanced electrostatic interaction, Biomacromolecules 16 (10) (2015) 3217–3225.
[92] S.R. Ali, Y. Ma, R.R. Parajuli, Y. Balogun, W.Y.C. Lai, H. He, A Nonoxidative sensor based on a self-doped polyaniline/carbon nanotube composite for sensitive and selective detection of the neurotransmitter dopamine, Anal. Chem. 79 (6) (2007) 2583–2587.
[93] S. Chen, G. Sun, High sensitivity ammonia sensor using a hierarchical polyaniline/poly(ethylene-co-glycidyl methacrylate) nanofibrous composite membrane, ACS Appl. Mater. Interfaces 5 (14) (2013) 6473–6477.
[94] R. Sha, K. Komori, S. Badhulika, Graphene-Polyaniline composite based ultrasensitive electrochemical sensor for non-enzymatic detection of urea, Electrochim. Acta 233 (2017) 44–51.
[95] J. Wu, L. Yin, Platinum nanoparticle modified polyaniline-functionalized boron

nitride nanotubes for amperometric glucose enzyme biosensor, ACS Appl. Mater. Interfaces 3 (11) (2011) 4354–4362.
[96] Y. Liu, X. Feng, J. Shen, J.-J. Zhu, W. Hou, Fabrication of a novel glucose biosensor based on a highly electroactive polystyrene/polyaniline/Au nanocomposite, J. Phys. Chem. C 112 (30) (2008) 9237–9242.
[97] M. Zhao, X. Wu, C. Cai, Polyaniline nanofibers: synthesis, characterization, and application to direct electron transfer of glucose oxidase, J. Phys. Chem. C 113 (12) (2009) 4987–4996.
[98] Z. Wang, S. Liu, P. Wu, C. Cai, Detection of glucose based on direct electron transfer reaction of glucose oxidase immobilized on highly ordered polyaniline nanotubes, Anal. Chem. 81 (4) (2009) 1638–1645.
[99] D. Wan, S. Yuan, G.L. Li, K.G. Neoh, E.T. Kang, Glucose biosensor from covalent immobilization of chitosan-coupled carbon nanotubes on polyaniline-modified gold electrode, ACS Appl. Mater. Interfaces 2 (11) (2010) 3083–3091.
[100] T.C. Bicak, M. Gicevičius, T.C. Gokoglan, G. Yilmaz, A. Ramanavicius, L. Toppare, Y. Yagci, Simultaneous and sequential synthesis of polyaniline-g-poly(ethylene glycol) by combination of oxidative polymerization and CuAAC click chemistry: a water-soluble instant response glucose biosensor material, Macromolecules 50 (5) (2017) 1824–1831.
[101] Z. Miao, P. Wang, A. Zhong, M. Yang, Q. Xu, S. Hao, X. Hu, Development of a glucose biosensor based on electrodeposited gold nanoparticles–polyvinylpyrrolidone–polyaniline nanocomposites, J. Electroanal. Chem. 756 (2015) 153–160.
[102] V. Mazeiko, A. Kausaite-Minkstimiene, A. Ramanaviciene, Z. Balevicius, A. Ramanavicius, Gold nanoparticle and conducting polymer-polyaniline-based nanocomposites for glucose biosensor design, Sens. Actuators B. Chem. 189 (2013) 187–193.
[103] C. Xiang, Y. Zou, S. Qiu, L. Sun, F. Xu, H. Zhou, Bienzymatic glucose biosensor based on direct electrochemistry of cytochrome c on gold nanoparticles/polyaniline nanospheres composite, Talanta 110 (2013) 96–100.
[104] X. Feng, H. Cheng, Y. Pan, H. Zheng, Development of glucose biosensors based on nanostructured graphene-conducting polyaniline composite, Biosens. Bioelectron. 70 (2015) 411–417.
[105] B. Hansen, M.A. Hocevar, C.A. Ferreira, A facile and simple polyaniline-poly (ethylene oxide) based glucose biosensor, Synth. Met. 222 (2016) 224–231.
[106] H. Chang, Y. Yuan, N. Shi, Y. Guan, Electrochemical DNA biosensor based on conducting polyaniline nanotube array, Anal. Chem. 79 (13) (2007) 5111–5115.
[107] Y. Bo, H. Yang, Y. Hu, T. Yao, S. Huang, A novel electrochemical DNA biosensor based on graphene and polyaniline nanowires, Electrochim. Acta 56 (6) (2011) 2676–2681.
[108] Q. Zhu, F. Gao, Y. Yang, B. Zhang, W. Wang, Z. Hu, Q. Wang, Electrochemical preparation of polyaniline capped Bi2S3 nanocomposite and its application in impedimetric DNA biosensor, Sens. Actuators B. Chem. 207 (2015) 819–826.
[109] J. Yang, X. Wang, H. Shi, An electrochemical DNA biosensor for highly sensitive detection of phosphinothricin acetyltransferase gene sequence based on polyaniline-(mesoporous nanozirconia)/poly-tyrosine film, Sens. Actuators B. Chem. 162 (1) (2012) 178–183.
[110] H. Deng, W. Shen, Y. Ren, Z. Gao, A highly sensitive microRNA biosensor based on hybridized microRNA-guided deposition of polyaniline, Biosens. Bioelectron. 60 (2014) 195–200.
[111] Z. Matharu, G. Sumana, S.K. Arya, S.P. Singh, V. Gupta, B.D. Malhotra, Polyaniline Langmuir – blodgett film based cholesterol biosensor, Langmuir 23 (26) (2007) 13188–13192.
[112] H. Zhang, R. Liu, J. Zheng, Seed-mediated synthesis of polyaniline/Au nanocomposite and its application for a cholesterol biosensor, Synth. Met. 167 (2013) 5–9.
[113] Y.J. Shin, J. Kameoka, Amperometric cholesterol biosensor using layer-by-layer adsorption technique onto electrospun polyaniline nanofibers, J. Ind. Eng. Chem. 18 (1) (2012) 193–197.
[114] B. Lakard, D. Magnin, O. Deschaume, G. Vanlancker, K. Glinel, S. Demoustier-Champagne, B. Nysten, A.M. Jonas, P. Bertrand, S. Yunus, Urea potentiometric enzymatic biosensor based on charged biopolymers and electrodeposited polyaniline, Biosens. Bioelectron. 26 (10) (2011) 4139–4145.
[115] C.C. Buron, M. Quinart, T. Vrlinic, S. Yunus, K. Glinel, A.M. Jonas, B. Lakard, Application of original assemblies of polyelectrolytes, urease and electrodeposited polyaniline as sensitive films of potentiometric urea biosensors, Electrochim. Acta 148 (2014) 53–61.
[116] S. Yadav, A. Kumar, C.S. Pundir, Amperometric creatinine biosensor based on covalently coimmobilized enzymes onto carboxylated multiwalled carbon nanotubes/polyaniline composite film, Anal. Biochem. 419 (2) (2011) 277–283.
[117] J. Luo, J. Huang, Y. Wu, J. Sun, W. Wei, X. Liu, Synthesis of hydrophilic and conductive molecularly imprinted polyaniline particles for the sensitive and selective protein detection, Biosens. Bioelectron. 94 (2017) 39–46.
[118] B. Batra, S. Kumari, C.S. Pundir, Construction of glutamate biosensor based on covalent immobilization of glutmate oxidase on polypyrrole nanoparticles/polyaniline modified gold electrode, Enzyme Microb. Technol. 57 (2014) 69–77.
[119] T.P. Tsele, A.S. Adekunle, O.E. Fayemi, E.E. Ebenso, Electrochemical detection of epinephrine using polyaniline nanocomposite films doped with TiO2 and RuO2 nanoparticles on multi-walled carbon nanotube, Electrochim. Acta 243 (2017) 331–348.
[120] N. Stasyuk, O. Smutok, G. Gayda, B. Vus, Y. Koval'chuk, M. Gonchar, Bi-enzyme l-arginine-selective amperometric biosensor based on ammonium-sensing polyaniline-modified electrode, Biosens. Bioelectron. 37 (1) (2012) 46–52.
[121] A. Fatoni, A. Numnuam, P. Kanatharana, W. Limbut, P. Thavarungkul, A conductive porous structured chitosan-grafted polyaniline cryogel for use as a sialic acid biosensor, Electrochim. Acta 130 (2014) 296–304.
[122] S.-W. Woo, K. Dokko, H. Nakano, K. Kanamura, Incorporation of polyaniline into macropores of three-dimensionally ordered macroporous carbon electrode for electrochemical capacitors, J. Power Sources 190 (2) (2009) 596–600.
[123] Y. Song, L. Jiang, W. Qi, C. Lu, X. Zhu, Fabrication of solid aluminum electrolytic capacitors utilizing conductive polyaniline solutions, Synth. Met. 162 (3–4) (2012) 368–374.
[124] Y. Jin, M. Fang, M. Jia, In situ one-pot synthesis of graphene–polyaniline nanofiber composite for high-performance electrochemical capacitors, Appl. Surf. Sci. 308 (2014) 333–340.
[125] M.S. Seyed Dorraji, I. Ahadzadeh, M.H. Rasoulifard, Chitosan/polyaniline/MWCNT nanocomposite fibers as an electrode material for electrical double layer capacitors, Int. J. Hydrogen Energy 39 (17) (2014) 9350–9355.
[126] W. Tang, L. Peng, C. Yuan, J. Wang, S. Mo, C. Zhao, Y. Yu, Y. Min, A.J. Epstein, Facile synthesis of 3D reduced graphene oxide and its polyaniline composite for super capacitor application, Synth. Met. 202 (2015) 140–146.
[127] P. Ningsih, C.Z. Holdsworth, S.W. Donne, The initial study of polyaniline with manganese oxides for electrochemical capacitors, Procedia Chem. 16 (2015) 540–547.
[128] N. Chen, Y. Ren, P. Kong, L. Tan, H. Feng, Y. Luo, In situ one-pot preparation of reduced graphene oxide/polyaniline composite for high-performance electrochemical capacitors, Appl. Surf. Sci. 392 (2017) 71–79.
[129] V.A. Demin, V.V. Erokhin, A.V. Emelyanov, S. Battistoni, G. Baldi, S. Iannotta, P.K. Kashkarov, M.V. Kovalchuk, Hardware elementary perceptron based on polyaniline memristive devices, Org. Electron. 25 (2015) 16–20.
[130] C.O. Baker, B. Shedd, R.J. Tseng, A.A. Martinez-Morales, C.S. Ozkan, M. Ozkan, Y. Yang, R.B. Kaner, Size control of gold nanoparticles grown on polyaniline nanofibers for bistable memory devices, ACS Nano 5 (5) (2011) 3469–3474.
[131] G. Yue, F. Tan, F. Li, C. Chen, W. Zhang, J. Wu, Q. Li, Enhanced performance of flexible dye-sensitized solar cell based on nickel sulfide/polyaniline/titanium counter electrode, Electrochim. Acta 149 (2014) 117–125.
[132] T.-T. Duong, T.Q. Tuan, D.V.A. Dung, N. Van Quy, D.-L. Vu, M.H. Nam, N.D. Chien, S.-G. Yoon, A.-T. Le, Application of polyaniline nanowires electrodeposited on the FTO glass substrate as a counter electrode for low-cost dye-sensitized solar cells, Curr. Appl. Phys. 14 (12) (2014) 1607–1611.
[133] S. Ghani, R. Sharif, S. Bashir, A. Ashraf, S. Shahzadi, A.A. Zaidi, S. Rafique, N. Zafar, A.H. Kamboh, Dye-sensitized solar cells with high-performance electrodeposited gold/polyaniline composite counter electrodes, Mater. Sci. Semicond. Process. 31 (2015) 588–592.
[134] G. Sai-Anand, A.-I. Gopalan, K.-P. Lee, S. Venkatesan, B.-H. Kang, S.-W. Lee, J.-S. Lee, Q. Qiao, D.-H. Kwon, S.-W. Kang, A futuristic strategy to influence the solar cell performance using fixed and mobile dopants incorporated sulfonated polyaniline based buffer layer, Sol. Energy Mater. Sol. Cells 141 (2015) 275–290.
[135] P. Yang, J. Duan, Q. Tang, Cobalt sulfide decorated polyaniline complex counter electrodes for efficient dye-sensitized solar cells, Electrochim. Acta 184 (2015) 64–69.
[136] K.-H. Park, S.J. Kim, R. Gomes, A. Bhaumik, High performance dye-sensitized solar cell by using porous polyaniline nanotubes as counter electrode, Chem. Eng. J. 260 (2015) 393–398.
[137] A. Bahramian, D. Vashaee, In-situ fabricated transparent conducting nanofiber-shape polyaniline/coral-like TiO2 thin film: application in bifacial dye-sensitized solar cells, Sol. Energy Mater. Sol. Cells 143 (2015) 284–295.
[138] K. Mohan, A. Bora, B.C. Nath, P. Gogoi, B.J. Saikia, S.K. Dolui, A highly stable and efficient quasi solid state dye sensitized solar cell based on Polymethyl methacrylate(PMMA)/Polyaniline Nanotube(PANI-NT) gel electrolyte, Electrochim. Acta 222 (2016) 1072–1078.
[139] R. Taş, M. Gülen, M. Can, S. Sönmezoğlu, Effects of solvent and copper-doping on polyaniline conducting polymer and its application as a counter electrode for efficient and cost-effective dye-sensitized solar cells, Synth. Met. 212 (2016) 75–83.
[140] Y. Yu, Q. Tang, B. He, H. Chen, Z. Zhang, L. Yu, Platinum alloy decorated polyaniline counter electrodes for dye-sensitized solar cells, Electrochim. Acta 190 (2016) 76–84.
[141] W. Hou, Y. Xiao, G. Han, D. Fu, R. Wu, Serrated, flexible and ultrathin polyaniline nanoribbons: an efficient counter electrode for the dye-sensitized solar cell, J. Power Sources 322 (2016) 155–162.
[142] J. Gao, Y. Yang, Z. Zhang, J. Yan, Z. Lin, X. Guo, Bifacial quasi-solid-state dye-sensitized solar cells with Poly (vinyl pyrrolidone)/polyaniline transparent counter electrode, Nano Energy 26 (2016) 123–130.
[143] K. Lee, K.H. Cho, J. Ryu, J. Yun, H. Yu, J. Lee, W. Na, J. Jang, Low-cost and efficient perovskite solar cells using a surfactant-modified polyaniline:poly(styrenesulfonate) hole transport material, Electrochim. Acta 224 (2017) 600–607.
[144] Y.-C. Shih, H.-L. Lin, K.-F. Lin, Electropolymerized polyaniline/graphene nanoplatelet/multi-walled carbon nanotube composites as counter electrodes for high performance dye-sensitized solar cells, J. Electroanal. Chem. 794 (2017) 112–119.
[145] B. He, X. Zhang, H. Zhang, J. Li, Q. Meng, Q. Tang, Transparent molybdenum sulfide decorated polyaniline complex counter electrodes for efficient bifacial dye-sensitized solar cells, Sol. Energy 147 (2017) 470–478.
[146] P. Hasin, V. Amornkitbamrung, N. Chanlek, Economical nanocomposites of cobalt or nickel species and polyaniline-derived N-doped mesoporous carbons for dye-sensitized solar cells as counter electrodes, J. Catal. 351 (2017) 19–32.
[147] C. Zhao, S. Xing, Y. Yu, W. Zhang, C. Wang, A novel all-plastic diode based upon pure polyaniline material, Microelectron. J. 38 (3) (2007) 316–320.
[148] K.-S. Kim, G.-S. Chung, Fabrication and characterization of surface type Schottky diode hydrogen sensor using polyaniline/porous 3C-SiC, Synth. Met. 162 (7–8) (2012) 636–640.
[149] A. Bera, K. Deb, V. Kathirvel, T. Bera, R. Thapa, B. Saha, Flexible diode of polyaniline/ITO heterojunction on PET substrate, Appl. Surf. Sci. 418 (Part A) (2017) 264–269.

[150] R.K. Pandey, C.S.S. Sandeep, R. Philip, V. Lakshminarayanan, Enhanced optical nonlinearity of polyaniline – porphyrin nanocomposite, J. Phys. Chem. C 113 (20) (2009) 8630–8634.
[151] K.K. Nagaraja, S. Pramodini, P. Poornesh, M.P. Telenkov, I.V. Kityk, Nonlinear optical properties of polyaniline and poly (o-toluidine) composite thin films with multi walled carbon nano tubes, Phys. B 512 (2017) 45–53.
[152] J.C.B. Santos, L.G. Paterno, E.A.T. Dirani, F.J. Fonseca, A.M. de Andrade, Influence of polyaniline and phthalocyanine hole-transport layers on the electrical performance of light-emitting diodes using MEH-PPV as emissive material, Thin Solid Films 516 (10) (2008) 3184–3188.
[153] J. Jang, J. Ha, K. Kim, Organic light-emitting diode with polyaniline-poly(styrene sulfonate) as a hole injection layer, Thin Solid Films 516 (10) (2008) 3152–3156.
[154] J.L. Alonso, J.C. Ferrer, M.A. Cotarelo, F. Montilla, S.F. de Ávila, Influence of the thickness of electrochemically deposited polyaniline used as hole transporting layer on the behavior of polymer light-emitting diodes, Thin Solid Films 517 (8) (2009) 2729–2735.
[155] H. Bejbouj, L. Vignau, J.L. Miane, T. Olinga, G. Wantz, A. Mouhsen, E.M. Oualim, M. Harmouchi, Influence of the nature of polyaniline-based hole-injecting layer on polymer light emitting diode performances, Mater. Sci. Eng. B 166 (3) (2010) 185–189.
[156] M. Mohsennia, M.M. Bidgoli, F.A. Boroumand, A.M. Nia, Electrically conductive polyaniline as hole-injection layer for MEH-PPV:BT based polymer light emitting diodes, Mater. Sci. Eng. B 197 (2015) 25–30.
[157] S. Bhadra, D. Khastgir, N.K. Singha, J.H. Lee, Progress in preparation, processing and applications of polyaniline, Prog. Polym. Sci. 34 (8) (2009) 783–810.
[158] A.G. MacDiarmid, "Synthetic Metals": a novel role for organic polymers (nobel lecture), Angew. Chem. Int. Ed. 40 (14) (2001) 2581–2590.
[159] N.V. Blinova, J. Stejskal, M. Trchová, J. Prokeš, Control of polyaniline conductivity and contact angles by partial protonation, Polym. Int. 57 (1) (2008) 66–69.
[160] H. Shirakawa, E.J. Louis, A.G. MacDiarmid, C.K. Chiang, A.J. Heeger, Synthesis of electrically conducting organic polymers: halogen derivatives of polyacetylene, (CH), J. Chem. Soc., Chem. Commun. 16 (1977) 578–580.
[161] G. Boara, M. Sparpaglione, Synthesis of polyanilines with high electrical conductivity, Synth. Met. 72 (2) (1995) 135–140.
[162] L. Dai, Intelligent macromolecules for smart devices: from materials synthesis to device applications, Springer Science & Business, Media (2004).
[163] T. Cortés María, C. Moreno Juan, Artificial muscles based on conducting polymers, e-Polymers (2003) 523.
[164] N.K. Guimard, N. Gomez, C.E. Schmidt, Conducting polymers in biomedical engineering, Prog. Polym. Sci. 32 (8–9) (2007) 876–921.
[165] J.L. Bredas, G.B. Street, Polarons, bipolarons, and solitons in conducting polymers, Acc. Chem. Res. 18 (10) (1985) 309–315.
[166] S. Sinha, S. Bhadra, D. Khastgir, Effect of dopant type on the properties of polyaniline, J. Appl. Polym. Sci. 112 (5) (2009) 3135–3140.
[167] D. Chandra Trivedi, S. Kumar, Dhawan, Investigations on the effect of 5-sulfosalicylic acid on the properties of polyaniline, Synth. Met. 58 (3) (1993) 309–324.
[168] G. Tzamalis, N.A. Zaidi, C.C. Homes, A.P. Monkman, Doping-dependent studies of the Anderson-Mott localization in polyaniline at the metal-insulator boundary, Phys. Rev. B 66 (8) (2002) 085202.
[169] S. Bhadra, S. Chattopadhyay, N.K. Singha, D. Khastgir, Improvement of conductivity of electrochemically synthesized polyaniline, J. Appl. Polym. Sci. 108 (1) (2008) 57–64.
[170] S. Bhadra, N.K. Singha, D. Khastgir, Polyaniline by new miniemulsion polymerization and the effect of reducing agent on conductivity, Synth. Met. 156 (16–17) (2006) 1148–1154.
[171] H. Bodugöz, O. Güven, Radiation induced dehydrochlorination as an in-situ doping technique for enhancement of the conductivity of polyaniline blends, Nucl. Instrum. Methods Phys. Res. Sect. B 236 (1–4) (2005) 153–159.
[172] P. Kiattibutr, L. Tarachiwin, L. Ruangchuay, A. Sirivat, J. Schwank, Electrical conductivity responses of polyaniline films to SO2–N2 mixtures: effect of dopant type and doping level, React. Funct. Polym. 53 (1) (2002) 29–37.
[173] E.R. Holland, S.J. Pomfret, P.N. Adams, L. Abell, A.P. Monkman, Doping dependent transport properties of polyaniline-CSA films, Synth. Met. 84 (1) (1997) 777–778.
[174] I. Yamaguchi, T. Nagano, L.V. Tuan, NaH-assisted n-doping of polyanilines with dopant cation trapping sites and their stability of n-doping state against air, Polymer 73 (2015) 79–85.
[175] C.-J. Chang, K.-W. Chu, ZnS/polyaniline composites with improved dispersing stability and high photocatalytic hydrogen production activity, Int. J. Hydrogen Energy 41 (46) (2016) 21764–21773.
[176] S. Bhadra, D. Khastgir, Degradation and stability of polyaniline on exposure to electron beam irradiation (structure–property relationship), Polym. Degrad. Stab. 92 (10) (2007) 1824–1832.
[177] I. Kulszewicz-Bajer, A. Proń, J. Abramowicz, C. Jeandey, J.-L. Oddou, J.W. Sobczak, Lewis acid doped polyaniline: preparation and spectroscopic characterization, Chem. Mater. 11 (3) (1999) 552–556.
[178] T. Jana, J. Chatterjee, A.K. Nandi, Sulfonic acid doped thermoreversible polyaniline gels. 3. structural investigations, Langmuir 18 (15) (2002) 5720–5727.
[179] Q. Yu, Crystal structure and property of proton acid and polypeptide co-doped polyaniline, J. Phys. Chem. C 120 (48) (2016) 27628–27634.
[180] T. Jana, A.K. Nandi, Sulfonic acid-doped thermoreversible polyaniline gels: morphological, structural, and thermodynamical investigations, Langmuir 16 (7) (2000) 3141–3147.
[181] J. Tarver, J.E. Yoo, T.J. Dennes, J. Schwartz, Y.-L. Loo, Polymer acid doped polyaniline is electrochemically stable beyond pH 9, Chem. Mater. 21 (2) (2009) 280–286.
[182] H. Gu, J. Guo, X. Zhang, Q. He, Y. Huang, H.A. Colorado, N. Haldolaarachchige, H. Xin, D.P. Young, S. Wei, Z. Guo, Giant magnetoresistive phosphoric acid doped polyaniline-silica nanocomposites, J. Phys. Chem. C 117 (12) (2013) 6426–6436.
[183] N. Abdul Rahman, M. Gizdavic-Nikolaidis, S. Ray, A.J. Easteal, J. Travas-Sejdic, Functional electrospun nanofibers of poly(lactic acid) blends with polyaniline or poly(aniline-co-benzoic acid), Synth. Met. 160 (17–18) (2010) 2015–2022.
[184] Z.F. Li, E. Ruckenstein, Grafting of poly(ethylene oxide) to the surface of polyaniline films through a chlorosulfonation method and the biocompatibility of the modified films, J. Colloid Interface Sci. 269 (1) (2004) 62–71.
[185] P.R. Bidez, S. Li, A.G. MacDiarmid, E.C. Venancio, Y. Wei, P.I. Lelkes, Polyaniline, an electroactive polymer, supports adhesion and proliferation of cardiac myoblasts, J. Biomater. Sci. Polym. Ed. 17 (1–2) (2006) 199–212.
[186] M. Li, Y. Guo, Y. Wei, A.G. MacDiarmid, P.I. Lelkes, Electrospinning polyaniline-contained gelatin nanofibers for tissue engineering applications, Biomaterials 27 (13) (2006) 2705–2715.
[187] H.-J. Wang, L.-W. Ji, D.-F. Li, J.-Y. Wang, Characterization of nanostructure and cell compatibility of polyaniline films with different dopant acids, J. Phys. Chem. C 112 (9) (2008) 2671–2677.
[188] S.I. Jeong, I.D. Jun, M.J. Choi, Y.C. Nho, Y.M. Lee, H. Shin, Development of electroactive and elastic nanofibers that contain polyaniline and poly(L-lactide-co-ε-caprolactone) for the control of cell adhesion, Macromol. Biosci. 8 (7) (2008) 627–637.
[189] H.-S. Kim, H.L. Hobbs, L. Wang, M.J. Rutten, C.C. Wamser, Biocompatible composites of polyaniline nanofibers and collagen, Synth. Met. 159 (13) (2009) 1313–1318.
[190] S. Liu, J. Wang, D. Zhang, P. Zhang, J. Ou, B. Liu, S. Yang, Investigation on cell biocompatible behaviors of polyaniline film fabricated via electroless surface polymerization, Appl. Surf. Sci. 256 (11) (2010) 3427–3431.
[191] M. Gizdavic-Nikolaidis, S. Ray, J.R. Bennett, A.J. Easteal, R.P. Cooney, Electrospun functionalized polyaniline copolymer-based nanofibers with potential application in tissue engineering, Macromol. Biosci. 10 (12) (2010) 1424–1431.
[192] W. Hu, S. Chen, Z. Yang, L. Liu, H. Wang, Flexible electrically conductive nanocomposite membrane based on bacterial cellulose and polyaniline, J. Phys. Chem. C 115 (26) (2011) 8453–8457.
[193] R.M. Moura, A.A.A. de Queiroz, Dendronized polyaniline nanotubes for cardiac tissue engineering, Artif. Organs 35 (5) (2011) 471–477.
[194] T.H. Qazi, R. Rai, D. Dippold, J.E. Roether, D.W. Schubert, E. Rosellini, N. Barbani, A.R. Boccaccini, Development and characterization of novel electrically conductive PANI–PGS composites for cardiac tissue engineering applications, Acta Biomater. 10 (6) (2014) 2434–2445.
[195] M.P. Prabhakaran, L. Ghasemi-Mobarakeh, G. Jin, S. Ramakrishna, Electrospun conducting polymer nanofibers and electrical stimulation of nerve stem cells, J. Biosci. Bioeng. 112 (5) (2011) 501–507.
[196] X. Zhang, J. Zhu, N. Haldolaarachchige, J. Ryu, D.P. Young, S. Wei, Z. Guo, Synthetic process engineered polyaniline nanostructures with tunable morphology and physical properties, Polymer 53 (10) (2012) 2109–2120.
[197] E.I. Yslas, L.E. Ibarra, D.O. Peralta, C.A. Barbero, V.A. Rivarola, M.L. Bertuzzi, Polyaniline nanofibers: acute toxicity and teratogenic effect on Rhinella arenarum embryos, Chemosphere 87 (11) (2012) 1374–1380.
[198] P. Humpolicek, V. Kasparkova, P. Saha, J. Stejskal, Biocompatibility of polyaniline, Synth. Met. 162 (7–8) (2012) 722–727.
[199] C.-W. Hsiao, M.-Y. Bai, Y. Chang, M.-F. Chung, T.-Y. Lee, C.-T. Wu, B. Maiti, Z.-X. Liao, R.-K. Li, H.-W. Sung, Electrical coupling of isolated cardiomyocyte clusters grown on aligned conductive nanofibrous meshes for their synchronized beating, Biomaterials 34 (4) (2013) 1063–1072.
[200] J. Stejskal, M. Hajná, V. Kašpárková, P. Humpolíček, A. Zhigunov, M. Trchová, Purification of a conducting polymer, polyaniline, for biomedical applications, Synth. Met. 195 (2014) 286–293.
[201] G. Thrivikraman, G. Madras, B. Basu, Intermittent electrical stimuli for guidance of human mesenchymal stem cell lineage commitment toward neural-like cells on electroconductive substrates, Biomaterials 35 (24) (2014) 6219–6235.
[202] J.C.-C. Wu, S. Ray, M. Gizdavic-Nikolaidis, B. Uy, S. Swift, J. Jin, R.P. Cooney, Nanostructured bioactive material based on polycaprolactone and polyaniline fiber-scaffolds, Synth. Met. 198 (2014) 41–50.
[203] N. Ucar, N. Kizildag, A. Onen, I. Karacan, O. Eren, Polyacrylonitrile-polyaniline composite nanofiber webs: effects of solvents, redoping process and dispersion technique, Fiber. Polym. 16 (10) (2015) 2223–2236.
[204] P. Humpolíček, Z. Kuceková, V. Kašpárková, J. Pelková, M. Modic, I. Junkar, M. Trchová, P. Bober, J. Stejskal, M. Lehocký, Blood coagulation and platelet adhesion on polyaniline films, Colloids Surf. B. Biointerfaces 133 (2015) 278–285.
[205] G. Thrivikraman, P.S. Lee, R. Hess, V. Haenchen, B. Basu, D. Scharnweber, Interplay of substrate conductivity, cellular microenvironment, and pulsatile electrical stimulation toward osteogenesis of human mesenchymal stem cells in vitro, ACS Appl. Mater. Interfaces 7 (41) (2015) 23015–23028.
[206] E.I. Yslas, P. Cavallo, D.F. Acevedo, C.A. Barbero, V.A. Rivarola, Cysteine modified polyaniline films improve biocompatibility for two cell lines, Mater. Sci. Eng. C 51 (2015) 51–56.
[207] N. Pramanik, K. Dutta, R.K. Basu, P.P. Kundu, Aromatic π-conjugated curcumin on surface modified polyaniline/polyhydroxyalkanoate based 3D porous scaffolds for tissue engineering applications, ACS Biomater. Sci. Eng. 2 (12) (2016) 2365–2377.
[208] P. Petrov, P. Mokreva, I. Kostov, V. Uzunova, R. Tzoneva, Novel electrically conducting 2-hydroxyethylcellulose/polyaniline nanocomposite cryogels: synthesis and application in tissue engineering, Carbohydr. Polym. 140 (2016) 349–355.
[209] Y. Li, X. Li, R. Zhao, C. Wang, F. Qiu, B. Sun, H. Ji, J. Qiu, C. Wang, Enhanced

adhesion and proliferation of human umbilical vein endothelial cells on conductive PANI-PCL fiber scaffold by electrical stimulation, Mater. Sci. Eng. C 72 (2017) 106–112.
[210] L. Mohammadi Amirabad, M. Massumi, M. Shamsara, I. Shabani, A. Amari, M. Mossahebi Mohammadi, S. Hosseinzadeh, S. Vakilian, S.K. Steinbach, M.R. Khorramizadeh, M. Soleimani, J. Barzin, Enhanced cardiac differentiation of human cardiovascular disease patient-specific induced pluripotent stem cells by applying unidirectional electrical pulses using aligned electroactive nanofibrous scaffolds, ACS Appl. Mater. Interfaces 9 (8) (2017) 6849–6864.
[211] J. Wei, S. Xiong, Y. Bai, P. Jia, J. Ma, X. Lu, Polyaniline nanoparticles doped with star-like poly(styrene sulfonate): synthesis and electrochromic properties, Sol. Energy Mater. Sol. Cells 99 (2012) 141–147.
[212] K. Qu, X. Zeng, Ionic liquid-doped polyaniline and its redox activities in the zwitterionic biological buffer MOPS, Electrochim. Acta 202 (2016) 73–83.
[213] J. Bhadra, N.K. Madi, N.J. Al-Thani, M.A. Al-Maadeed, Polyaniline/polyvinyl alcohol blends: effect of sulfonic acid dopants on microstructural, optical, thermal and electrical properties, Synth. Met. 191 (2014) 126–134.
[214] G. Ravi Kumar, J. Vivekanandan, A. Mahudeswaran, P.S. Vijayanand, Synthesis and characterization of novel poly(aniline-co-m-aminoacetophenone) copolymer nanocomposites using dodecylbenzene sulfonic acid as a soft template, Iran. Polym. J. 22 (12) (2013) 923–929.
[215] T. Amaya, R. Sugihara, D. Hata, T. Hirao, Self-doped polyaniline derived from poly (2-methoxyaniline-5-phosphonic acid) and didodecyldimethylammonium salt, RSC Adv. 6 (27) (2016) 22447–22452.
[216] N.V. Blinova, M. Trchová, J. Stejskal, The polymerization of aniline at a solution–gelatin gel interface, Eur. Polym. J. 45 (3) (2009) 668–673.
[217] K.C. Dee, D.A. Puleo, R. Bizios, Biocompatibility, An Introduction To Tissue-Biomaterial Interactions, John Wiley & Sons, Inc., 2003, pp. 173–184.
[218] J.M. Anderson, F.J. Schoen, In Vivo Assessment of Tissue Compatibility, Biomaterials Science, third ed., Academic Press, 2013, pp. 609–617 (Chapter II.3.4).
[219] L. Shadi, M. Karimi, S. Ramazani, A.A. Entezami, Preparation of electrospun nanofibers of star-shaped polycaprolactone and its blends with polyaniline, J. Mater. Sci. 49 (14) (2014) 4844–4854.
[220] D.J.C. Gomes, N.C. de Souza, J.R. Silva, Using a monocular optical microscope to assemble a wetting contact angle analyzer, Measurement 46 (9) (2013) 3623–3627.
[221] C.H. Wang, Y.Q. Dong, K. Sengothi, K.L. Tan, E.T. Kang, In-vivo tissue response to polyaniline, Synth. Met. 102 (1–3) (1999) 1313–1314.
[222] S. Kamalesh, P. Tan, J. Wang, T. Lee, E.-T. Kang, C.-H. Wang, Biocompatibility of electroactive polymers in tissues, J. Biomed. Mater. Res. 52 (3) (2000) 467–478.
[223] T.H. Qazi, R. Rai, A.R. Boccaccini, Tissue engineering of electrically responsive tissues using polyaniline based polymers: a review, Biomaterials 35 (33) (2014) 9068–9086.
[224] H. Miyoshi, Smart Design of Materials for Tissue Engineering, Smart Materials for Tissue Engineering: Fundamental Principles, The Royal Society of Chemistry, 2017, pp. 1–24 (Chapter 1).
[225] L. Wang, X. Li, Y.H. Tsou, X.Y. Xu, Applications of Conductive Materials for Tissue Engineering, Smart Materials for Tissue Engineering: Applications, The Royal Society of Chemistry, 2017, pp. 110–143 (Chapter 5).
[226] C.E. Schmidt, V.R. Shastri, J.P. Vacanti, R. Langer, Stimulation of neurite outgrowth using an electrically conducting polymer, Proc. Natl. Acad. Sci. 94 (17) (1997) 8948–8953.
[227] Z. Zhang, M. Rouabhia, Z. Wang, C. Roberge, G. Shi, P. Roche, J. Li, L.H. Dao, Electrically conductive biodegradable polymer composite for nerve regeneration: electricity-stimulated neurite outgrowth and axon regeneration, Artif. Organs 31 (1) (2007) 13–22.
[228] M. Kabiri, M. Soleimani, I. Shabani, K. Futrega, N. Ghaemi, H.H. Ahvaz, E. Elahi, M.R. Doran, Neural differentiation of mouse embryonic stem cells on conductive nanofiber scaffolds, Biotechnol. Lett. 34 (7) (2012) 1357–1365.
[229] S. Meng, Nerve cell differentiation using constant and programmed electrical stimulation through conductive non-functional graphene nanosheets film, Tissue Eng. Regener. Med. 11 (4) (2014) 274–283.
[230] J.-O. You, M. Rafat, G.J.C. Ye, D.T. Auguste, Nanoengineering the heart: conductive scaffolds enhance connexin 43 expression, Nano Lett. 11 (9) (2011) 3643–3648.
[231] N. Tandon, A. Marsano, R. Maidhof, L. Wan, H. Park, G. Vunjak-Novakovic, Optimization of electrical stimulation parameters for cardiac tissue engineering, J. Tissue Eng. Regen. Med. 5 (6) (2011) e115–e125.
[232] M.N. Hirt, J. Boeddinghaus, A. Mitchell, S. Schaaf, C. Börnchen, C. Müller, H. Schulz, N. Hubner, J. Stenzig, A. Stoehr, C. Neuber, A. Eder, P.K. Luther, A. Hansen, T. Eschenhagen, Functional improvement and maturation of rat and human engineered heart tissue by chronic electrical stimulation, J. Mol. Cell. Cardiol. 74 (2014) 151–161.
[233] P.R. Bidez, J.Y. Kresh, Y. Wei, P.I. Lelkes, Enhanced cardiac differentiation of mouse embryonic stem cells by electrical stimulation, in: G.M. Artmann, S. Minger, J. Hescheler (Eds.), Stem Cell Engineering: Principles and Applications, Springer, Berlin Heidelberg, Berlin, Heidelberg, 2011, pp. 119–141.
[234] F. Pires, Q. Ferreira, C.A.V. Rodrigues, J. Morgado, F.C. Ferreira, Neural stem cell differentiation by electrical stimulation using a cross-linked PEDOT substrate: expanding the use of biocompatible conjugated conductive polymers for neural tissue engineering, Biochim. Biophys. Acta Gen. Subj. 1850 (6) (2015) 1158–1168.
[235] X. Gu, J. Fu, J. Bai, J. Wang, W. Pan, C. Zhang, Low-frequency electrical stimulation induces the proliferation and differentiation of peripheral blood stem cells into schwann cells, Am. J. Med. Sci. 349 (2) (2015) 157–161.
[236] E. Serena, E. Figallo, N. Tandon, C. Cannizzaro, S. Gerecht, N. Elvassore, G. Vunjak-Novakovic, Electrical stimulation of human embryonic stem cells: cardiac differentiation and the generation of reactive oxygen species, Exp. Cell Res. 315 (20) (2009) 3611–3619.
[237] Y. Min, Y. Liu, Y. Poojari, J.-C. Wu, B.E. Hildreth Iii, T.J. Rosol, A.J. Epstein, Self-doped polyaniline-based interdigitated electrodes for electrical stimulation of osteoblast cell lines, Synth. Met. 198 (2014) 308–313.
[238] Y. Min, Y. Yang, Y. Poojari, Y. Liu, J.-C. Wu, D.J. Hansford, A.J. Epstein, Sulfonated polyaniline-based organic electrodes for controlled electrical stimulation of human osteosarcoma cells, Biomacromolecules 14 (6) (2013) 1727–1731.
[239] J. Zhang, K. Qiu, B. Sun, J. Fang, K. Zhang, H. Ei-Hamshary, S.S. Al-Deyab, X. Mo, The aligned core-sheath nanofibers with electrical conductivity for neural tissue engineering, J. Mater. Chem. B 2 (45) (2014) 7945–7954.
[240] L. Wang, Q. Huang, J.-Y. Wang, Nanostructured polyaniline coating on ITO glass promotes the neurite outgrowth of PC 12 cells by electrical stimulation, Langmuir 31 (44) (2015) 12315–12322.
[241] S.H. Ku, S.H. Lee, C.B. Park, Synergic effects of nanofiber alignment and electroactivity on myoblast differentiation, Biomaterials 33 (26) (2012) 6098–6104.
[242] J.G. Hardy, J.Y. Lee, C.E. Schmidt, Biomimetic conducting polymer-based tissue scaffolds, Curr. Opin. Biotechnol. 24 (5) (2013) 847–854.